containing 10% FBS. Then the medium was changed and 5.5 μl of polyplex was added to each well similarly as in the transfection described above. After 4, 8, or 24 h, the plates were centrifuged for 5 min at 110*g*. Then, 50 μl of aliquots in each well were collected and subjected to the LDH measurement. A CytoTox 96 Non-Radioactive Cytotoxicity Assay kit (Promega) was used following the protocol provided by the manufacturer, using a plate reader AD200 (Beckman Coulter, Inc., USA) for reading the OD at 490 nm to determine the amount of the produced diformazan. Freeze-chaw cells were used to calibrate 100% LDH activity. To compare the cytotoxicity between P[Asp(DET)] and LPEI, the parametrical analysis using the Student's *t*-test was performed.

2.8. Quantitative assay on the cellular uptake of pDNA by real-time quantitative PCR

EGFP-C1 pDNA expressing EGFP was transfected to HuH-7. 8×10^4 HuH-7 cells/well were plated in six-well plates and cultured overnight, and then the transfection was done similarly as described before. At the indicated time periods (4, 8 and 24 h), the DNA was collected and purified from each well using a Wizard Genomic DNA purification Kit (Promega), then subjected to the PCR for the quantification of pDNA copies encoding EGFP. The copy number of β-actin (βA) was also determined by the ABI 7500 Fast Real-Time PCR systems to normalize the cell number (Applied Biosystems, Foster City, CA, USA). The sequences of the primers and probe used for EGFP were as follows: forward primer GGGCACAAGCTGGAGTACAAC and reverse primer TCTGCTT GTCGGCCATGATA. The sequence of the probe was ACAGCCA CAACGTCT with FAM as a fluorescent dye on the 5-end and MGB as a fluorescence quencher dye labeled on the 3-end. For βA amplification and quantitation, the forward and reverse primers and probe were purchased as a standard TaqMan gene expression assay kit from Applied Biosystems. PCR was done for 20 s at 95 °C, followed by 3 s at 95 °C and 60 s at 60 °C for 40 cycles. A linear relationship between the number of cells and threshold cycle for the βA gene amplification was confirmed (data not shown).

2.9. Evaluation of osteocalcin mRNA expression

Osteogenic differentiation of the mouse calvarial cells was evaluated by the expression of osteocalcin mRNA, an osteoblast-differentiation marker. Mouse calvarial cells were isolated from the calvariae of neonatal littermates. The experimental procedures were handled in accordance with the guidelines of the Animal Committee of the University of Tokyo. Calvariae were digested for 10 min at 37–8 °C in an enzyme solution containing 0.1% collagenase and 0.2% dispase for five cycles. Cells isolated by the final four digestions were combined and cultured in DMEM supplemented with 10% FBS and penicillin/streptomycin. For induction of the differentiation assays, 3×10^4 primary mouse calvarial cells were plated in six-well culture plates and cultured for 24 h. After changing the medium to that containing 10% FBS and dexamethazone, polyplexes containing pDNAs expressing caALK6 and Runx2 were applied to each well by a similar transfection procedure as that previously described. The culture medium was refreshed on Day 3 after transfection, then changed every 3 days. On Days 5 and 11, the cells were washed with PBS and the total RNA was collected using the RNeasy Mini Preparation Kit (Qiagen) according to the manufacturer's protocol. Gene expression was analyzed by a quantitative PCR. 500 ng of total RNA was analyzed in a final volume of 50 μl. Reverse transcription was performed for 30 min at 50 °C followed by PCR: 50 °C for 2 min, 95 °C for 10 min, followed by 40 cycles of 95 °C for 15 s and 60 °C for 1 min using the Quantitect SYBR Green PCR Kit (Qiagen). Each mRNA expression was normalized to levels of mouse βA mRNA. The primers used were as follows: osteocalcin: forward primer (AAGCAGGAGGGCAATAAGGT) and reverse primer (TTTGTAGGCGGTCTTCAAGC); mouse βA: forward primer (AGATGTGGATCAGCAAGCAG), reverse primer (GCGCAAGT-TAGGTTTTGTCA). To compare the osteocalcin expressions using P[Asp(DET)] or LPEI, the parametrical analysis using the Student's *t*-test was performed.

2.10. Housekeeping gene expression assay

After a similar transfection procedure as previously described was performed, the total RNA was collected at 24 or 72 h. To evaluate the expressions of the housekeeping genes, a Taqman Human Endogenous Control Plate (Applied Biosystems) was used according to the manufacturer's protocol, including 18S rRNA, acidic ribosomal protein (PO), βA, cyclophilin (CYC), glyceraldehyde-3-phosphate dehydrogenase (GAPDH), phosphoglycero-kinase (PGK), β2-microglobulin (β2m), β-glucronidase (GUS), hypoxanthine ribosyl transferase (HPRT), TATA binding protein (TBP) and transferrin receptor (TfR). The control cells serve as a baseline for the assays and are shown as zero on the graph. The results are expressed in the comparative cycle threshold; ΔC_T, greater than or less than the control ΔC_T.

3. Results and discussion

3.1. In vitro transfection toward bioluminescent cell line

The bioluminescent human hepatoma cell line (HuH-7-Luc) stably expressing firefly luciferase (Luc) was used to evaluate the pharmacogenomic influence as well as the transfection efficiency of the polyplexes. After the transfection of RL using P[Asp(DET)] or LPEI, both the Luc and RL expressions were estimated simultaneously. The expressions were normalized by the number of cells, which were directly counted after scraping the cells from the culture plates.

The exogenous RL expressions per cell in Fig. 1(a) showed that the P[Asp(DET)] polyplex had comparable transfection efficiency to the LPEI polyplex giving the highest expression at 48 h after transfection. In contrast, the endogenous Luc expression showed a different profile between the two polyplexes; the Luc expression of the cells transfected by the P[Asp(DET)] polyplex was equivalent as that of the control cells, while the cells transfected by the LPEI polyplex showed a gradual decrease in Luc expression per cell (Fig. 1(b)). The cell numbers shown in Fig. 1(c) revealed that the proliferation was significantly inhibited by the transfection using LPEI after Day 2, compared to that of the other two groups (the cells transfected by P[Asp(DET)] and the control). Note that in these experiments, the polyplexes in the medium were removed at 24 h after transfection by changing the culture medium. Thus, these results suggest that although the exogenous RL gene expression showed an increase until Day 2, the internalized LPEI into the target cells by Day 1 had some continuous inhibiting effects on the proliferation and endogenous gene expression in the targeted cells. It is reasonable to assume that the LPEI released from the polyplex may impair the intracellular activities in a time-dependent manner.

3.2. Investigation of the cytotoxicity induced by LPEI

To investigate the detailed mechanisms of the time-dependent cytotoxicity possibly induced by LPEI, we

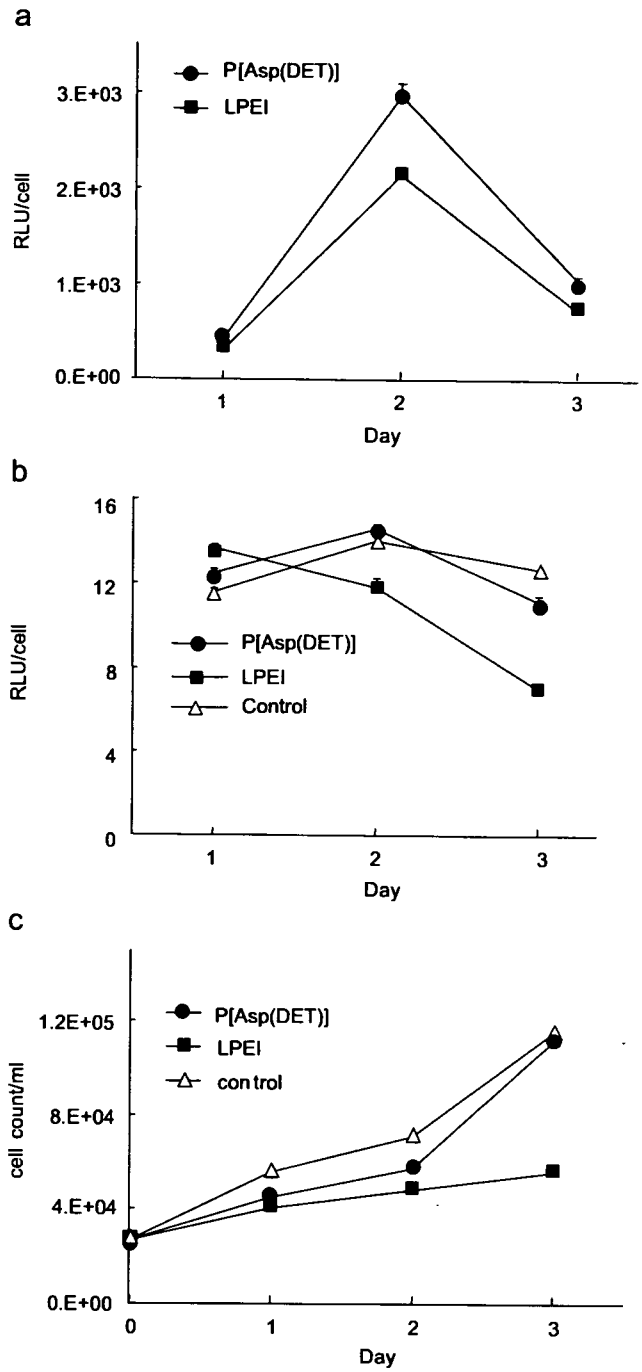

Fig. 1. *In vitro* transfection toward HuH-7-Luc cells. (a) Exogenous renilla luciferase expression. (b) Endogenous firefly luciferase expression. (c) Cell proliferation assay. Transfection was performed by P[Asp(DET)] (closed circle) or LPEI (closed square) polyplexes formed at $N/P = 10$. Gene expression was evaluated for 3 days after transfection and normalized by the cell number. Each data of gene expression represents mean ± SD ($n = 8$). The data of cell number are means ($n = 2$).

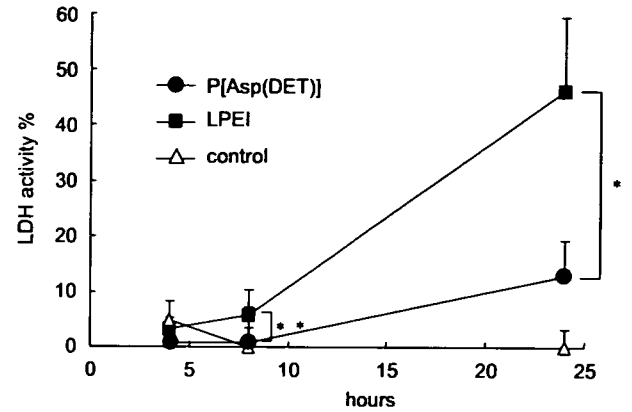

Fig. 2. Evaluation of LDH activity after transfecton using P[Asp(DET)] (closed circle) or LPEI (closed square) polyplexes. Each data represents mean ± SD ($n = 8$). Freeze-chaw cells were used to calibrate 100% LDH activity. $^{**}P<0.01$.

further assessed each step involved in the transfection process. The first step is apparently the cellular association and internalization of the gene carriers. It is assumed that these events may evoke membrane destabilization, possibly causing cytotoxic effects [15]. The change in membrane permeability due to the interaction with the polyplexes was examined by an LDH assay under the same condition as used in the transfection experiments above. As presented in Fig. 2, the cells transfected by the LPEI polyplex revealed a time-dependent increase in the leakage of LDH until 24 h after transfection. In contrast, the P[Asp(DET)] polyplex induced a minimal LDH leakage compared to the control. Considering the similar cationic nature of LPEI and P[Asp(DET)], the membrane destabilization after their association onto the plasma membrane is expected to be similar, which is apparently not the case observed here. The discrepancy between the two polymers on the time-dependent LDH leakage suggests that factors other than simple electrostatic interaction play a substantial role in the process of membrane destabilization.

The uptake amount of reporter gene into the HuH-7 cells by the P[Asp(DET)] or LPEI polyplex was determined by a real-time PCR in terms of gene copies per cell from the total DNA samples [16–18]. As seen in Fig. 3(a), the uptake amount of reporter gene showed a continuous increase until 24 h after the transfection in the case of the P[Asp(DET)] polyplex. The amount of reporter genes internalized with the LPEI polyplex was similar to that with the P[Asp(DET)] polyplex at 8 h, yet was significantly reduced by extending the transfection time to 24 h. One possible reason for this phenomenon might be the rapid dissociation of pDNA from LPEI in the cytoplasm as reported in the literature [19], resulting in its fast degradation by cytoplasmic enzymes [20,21]. However, when the culture medium was changed to remove the polyplexes at 4 h after the transfection, both systems showed a similar profile of a gradual decrease in the copy number after the medium change (Fig. 3(b)), suggesting the similar stability of the internalized pDNAs for both systems. These results suggest that the decrease in the internalized amount of the reporter gene with the LPEI polyplex shown in Fig. 3(a) may be due to

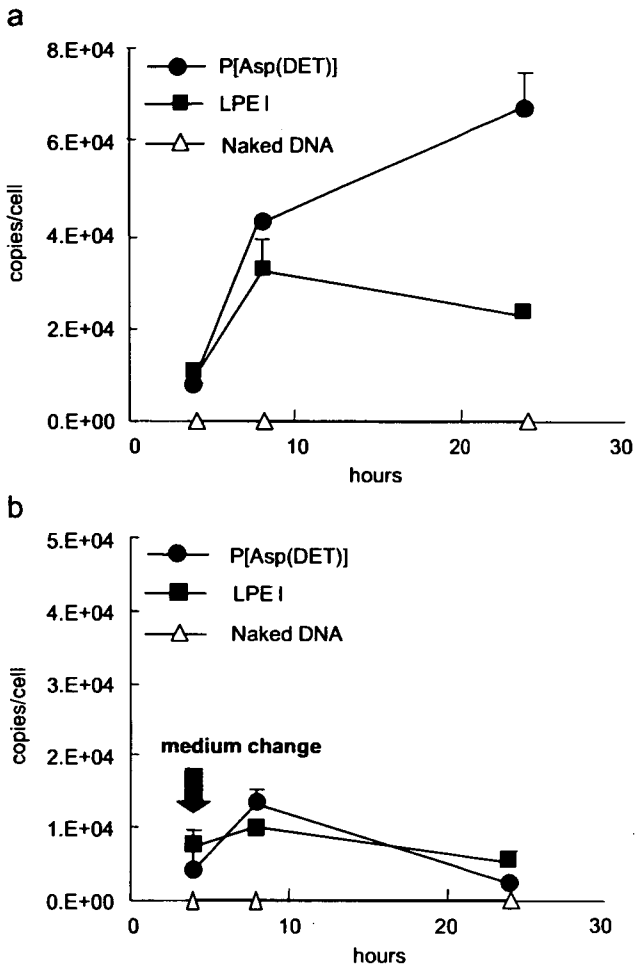

Fig. 3. Evaluation of pDNA uptake after transfecton using P[Asp(DET)] (closed circle), LPEI (closed square), or by the form of naked pDNA (open triangle). The cellular uptake of pDNA was quantified by a PCR, (a) without changing medium during the procedure, or (b) with medium change after 4 h of transfection. Each data represents mean ± SD ($n = 3$).

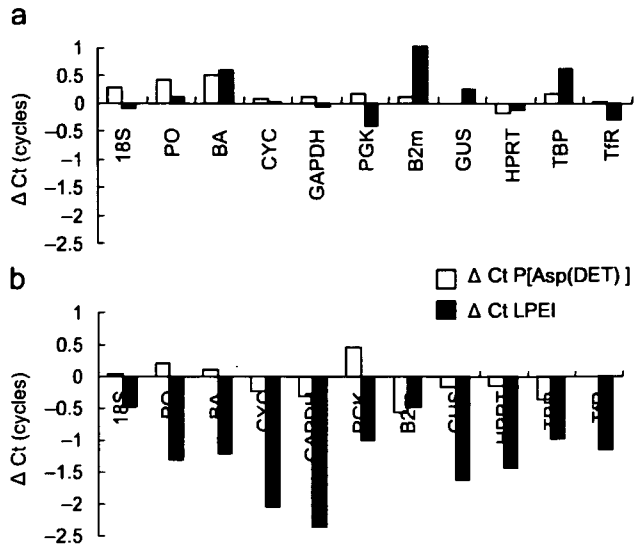

Fig. 4. Housekeeping genes expression after transfection. The mRNA expressions of various housekeeping genes were evaluated by a quantitative PCR at (a) 24 h and (b) 72 h after transfection using P[Asp(DET)] (open bar) or LPEI (filled bar).

the time-dependent decrease in the cellular activity to take up the polyplexes caused by the toxicity of LPEI.

To clarify this possible time-dependent influence on the cellular function from the viewpoint of the genomics, we assessed the change in the gene expressions of 11 frequently used housekeeping genes in the presence of the polyplex. These genes usually revealed a uniform expression, but the expression profile may vary in response to various external factors such as stress on the cells [22,23]. Thus, the variation in their expression profile is a good indicator for assessing the cellular function, a possible perturbation in the cellular homeostasis. The quantitative evaluation of the expression of these housekeeping genes by a real-time PCR revealed that the cells transfected by LPEI apparently showed downregulation in the expression of the housekeeping genes at 72 h after the transfection (Fig. 4(b)). Although the measurement at 24 h showed minimal fluctuation in the housekeeping gene expression, GAPDH and CYC were significantly downregulated by more than two cycles of ΔC_T values compared to those of the control cells at 72 h, indicating a four-fold decrease in gene expression. In these assays, the culture medium was changed at 24 h. Thus, it is likely that LPEI associated with the cells may induce the perturbed gene expression through the continuous interaction with intracellular components even after the medium change at 24 h to remove excess polyplexes in the medium. In contrast, the expression of these genes in the cells transfected by P[Asp(DET)] retained constant even after 72 h, all of which were within 0.5 cycles compared to those of the control cells. These results of the housekeeping gene expressions suggest the sustained homeostasis through the transfection process using P[Asp(DET)], leading to constant cellular activity such as the polyplex uptake (Fig. 3(a)), proliferation (Fig. 1(c)), and continuous gene expression (Fig. 1(b)).

As was occasionally reported, polyplexes induce critical cytotoxicity especially at higher N/P ratios, presumably due to the presence of free polymers [24–26]. Although the mechanisms are likely to involve various cellular responses such as immunostimulation [27] and apoptosis [15,28], the plasma membrane perturbation associated with the cationic polymers may be an initial event that induces the toxicity [28,29]. From our present results on LDH release (Fig. 2), the disorder on the plasma membrane seems to occur within 24 h after the transfection with the LPEI polyplex. In addition, the intracellular events that were noticed as the change in the endogenous gene expressions emerged after 72 h of transfection. It should be noted that these events of the perturbed expression of endogenous genes were inevitable even after further supply of the polyplexes was halted by the medium change at 24 h, strongly suggesting that the free PEI remaining inside the

cells after the polyplex dissociation may cause an unfavorable interaction with the intracellular components in a time-dependent manner.

3.3. Transfection toward mouse calvarial cells and induction of osteogenic differentiation

The data so far indicates the minimal cytotoxicity of P[Asp(DET)], suggesting a feasible capacity in gene delivery for therapeutic purposes. To assess this feasibility, we evaluated the induction of cell differentiation by exogenous gene introduction. pDNAs encoding bioactive factors, caALK6 and Runx2, both of which were revealed to induce the effective osteogenic differentiation [30], were introduced in this way to mouse calvarial cells derived from neonatal calvariae. The osteogenic differentiation was evaluated by the expression of osteocalcin mRNA, a specific osteoblast-differentiation marker. As shown in Fig. 5, the time-dependent increase in osteocalcin expression was confirmed after the transfection of caALK6+ Runx2 using P[Asp(DET)]. In contrast, no sign of the osteocalcin expression was observed by the LPEI polyplex until Day 11. Notably, the GFP-encoding pDNA, a negative control of differentiation, achieved almost identical GFP expression by the P[Asp(DET)] and LPEI polyplexes, without apparent morphologic changes in the targeted cells as observed under the microscope (data not shown). It can be reasonably assumed that, with the same transfection procedure, the osteogenic factors of caALK6 and Runx2 were also expressed similarly inside the targeted cells by the P[Asp(DET)] and LPEI polyplexes. Therefore, the lack of osteocalcin induction by the LPEI polyplex is considered to be due to the adverse effect on cell bioactivity by LPEI. In contrast, P[Asp(DET)] was revealed to be available for practical use in the induction of cell differentiation.

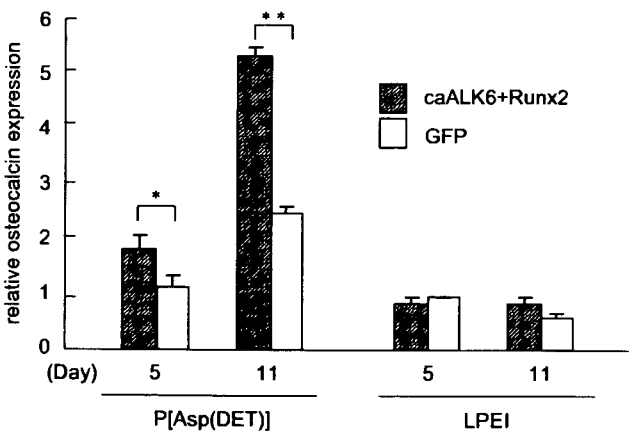

Fig. 5. Evaluation of osteocalcin mRNA expression by a quantitative PCR. Osteogenic differentiation was induced on the mouse calvarial cells by transfection of caALK6 and Runx2 (hatched bar) using P[Asp(DET)] or LPEI. As a negative control, a GFP (open bar) gene was used. After 5 or 11 days of transfection, the total RNA was collected and the osteocalcin expression was estimated. Each data represents mean±SD ($n = 3$). *$P<0.05$ and **$P<0.01$.

4. Conclusions

In conclusion, although LPEI has been widely used for gene introduction to various cell lines, the time-dependent cytotoxicity, which perturbs cellular homeostasis, should be carefully considered even though an appreciable expression of the reporter gene was achieved. As exemplified here in the osteogenic differentiation, impaired cellular function gave a negative effect in the intracellular signal transduction directing cell differentiation. This aspect of toxicity should be carefully counted especially when gene therapy is proposed to promote such cell functions as differentiation. Worth noting in this regard is the excellent capacity of the gene introduction of P[Asp(DET)] with minimal toxic effects, indicating that this system holds much promise for the therapeutic applications of gene therapy requiring safe and regulated gene expressions.

Acknowledgments

We thank Dr. M. Krüppel and Dr. K. Miyazono for pDNAs expressing caALK6 and Runx2, respectively. This work was supported by Grants-in-Aid for Scientific Research from the Japanese Ministry of Education, Culture, Sports, Science and Technology (#15390452 and #17390412), Health Science Research Grants from the Japanese Ministry of Health, Labor and Welfare (#H17-Immunology-009), and the Core Research Program for Evolutional Science and Technology (CREST) from the Japan Science and Technology (JST) Agency.

References

[1] Marshall E. Gene therapy death prompts review of adenovirus vector. Science 1999;286(5448):2244–5.
[2] Hollon T. Researchers and regulators reflect on first gene therapy death. Nat Med 2000;6(1):6.
[3] Assessment of adenoviral vector safety and toxicity: report of the National Institutes of Health Recombinant DNA advisory committee. Hum Gene Ther 2002;13(1):3–13.
[4] Gansbacher B. Report of a second serious adverse event in a clinical trial of gene therapy for X-linked severe combined immune deficiency (X-SCID). Position of the European Society of Gene Therapy (ESGT). J Gene Med 2003;5(3):261–2.
[5] Mosmann T. Rapid colorimetric assay for cellular growth and survival: application to proliferation and cytotoxicity assays. J Immunol Methods 1983;65(1–2):55–63.
[6] Duncan R. The dawning era of polymer therapeutics. Nat Rev Drug Discov 2003;2(5):347–60.
[7] Omidi Y, Hollins AJ, Benboubetra M, Drayton R, Benter IF, Akhtar S. Toxicogenomics of non-viral vectors for gene therapy: a microarray study of lipofectin- and oligofectamine-induced gene expression changes in human epithelial cells. J Drug Target 2003;11(6):311–23.
[8] Kabanov AV, Batrakova EV, Sriadibhatla S, Yang Z, Kelly DL, Alakov VY. Polymer genomics: shifting the gene and drug delivery paradigms. J Control Release 2005;101(1-3):259–71.

[9] Kanayama N, Fukushima S, Nishiyama N, Itaka K, Jang WD, Miyata K, et al. A PEG-based biocompatible block catiomer with high buffering capacity for the construction of polyplex micelles showing efficient gene transfer toward primary cells. Chem Med Chem 2006;1(4):439–44.
[10] Boussif O, Lezoualc'h F, Zanta MA, Mergny MD, Scherman D, Demeneix B, et al. A versatile vector for gene and oligonucleotide transfer into cells in culture and in vivo: polyethylenimine. Proc Natl Acad Sci USA 1995;92(16):7297–301.
[11] Boletta A, Benigni A, Lutz J, Remuzzi G, Soria MR, Monaco L. Nonviral gene delivery to the rat kidney with polyethylenimine. Hum Gene Ther 1997;8(10):1243–51.
[12] Goula D, Benoist C, Mantero S, Merlo G, Levi G, Demeneix BA. Polyethylenimine-based intravenous delivery of transgenes to mouse lung. Gene Ther 1998;5(9):1291–5.
[13] Akagi D, Oba M, Koyama H, Nishiyama N, Fukushima S, Miyata T, et al. Biocompatible micellar nanovectors achieve efficient gene transfer to vascular lesions without cytotoxicity and thrombus formation. Gene Ther 2007;14(13):1029–38.
[14] Itaka K, Ohba S, Chung U, Kataoka K. Bone regeneration by regulated in vivo gene transfer using biocompatible polyplex nanomicelles. Mol Ther 2007; Epub ahead of print.
[15] Moghimi SM, Symonds P, Murray JC, Hunter AC, Debska G, Szewczyk A. A two-stage poly(ethylenimine)-mediated cytotoxicity: implications for gene transfer/therapy. Mol Ther 2005;11(6):990–5.
[16] Lehmann MJ, Sczakiel G. Spontaneous uptake of biologically active recombinant DNA by mammalian cells via a selected DNA segment. Gene Ther 2005;12(5):446–51.
[17] Varga CM, Tedford NC, Thomas M, Klibanov AM, Griffith LG, Lauffenburger DA. Quantitative comparison of polyethylenimine formulations and adenoviral vectors in terms of intracellular gene delivery processes. Gene Ther 2005;12(13):1023–32.
[18] Hama S, Akita H, Ito R, Mizuguchi H, Hayakawa T, Harashima H. Quantitative comparison of intracellular trafficking and nuclear transcription between adenoviral and lipoplex systems. Mol Ther 2006;13(4):786–94.
[19] Itaka K, Harada A, Yamasaki Y, Nakamura K, Kawaguchi H, Kataoka K. In situ single cell observation by fluorescence resonance energy transfer reveals fast intra-cytoplasmic delivery and easy release of plasmid DNA complexed with linear polyethylenimine. J Gene Med 2004;6(1):76–84.
[20] Goncalves C, Pichon C, Guerin B, Midoux P. Intracellular processing and stability of DNA complexed with histidylated polylysine conjugates. J Gene Med 2002;4(3):271–81.
[21] Lechardeur D, Sohn KJ, Haardt M, Joshi PB, Monck M, Graham RW, et al. Metabolic instability of plasmid DNA in the cytosol: a potential barrier to gene transfer. Gene Ther 1999;6(4): 482–97.
[22] Thellin O, Zorzi W, Lakaye B, De Borman B, Coumans B, Hennen G, et al. Housekeeping genes as internal standards: use and limits. J Biotechnol 1999;75(2-3):291–5.
[23] Jain M, Nijhawan A, Tyagi AK, Khurana JP. Validation of housekeeping genes as internal control for studying gene expression in rice by quantitative real-time PCR. Biochem Biophys Res Commun 2006;345(2):646–51.
[24] Godbey WT, Wu KK, Mikos AG. Poly(ethylenimine)-mediated gene delivery affects endothelial cell function and viability. Biomaterials 2001;22(5):471–80.
[25] Morimoto K, Nishikawa M, Kawakami S, Nakano T, Hattori Y, Fumoto S, et al. Molecular weight-dependent gene transfection activity of unmodified and galactosylated polyethyleneimine on hepatoma cells and mouse liver. Mol Ther 2003;7(2):254–61.
[26] Boeckle S, von Gersdorff K, van der Piepen S, Culmsee C, Wagner E, Ogris M. Purification of polyethylenimine polyplexes highlights the role of free polycations in gene transfer. J Gene Med 2004; 6(10):1102–11.
[27] Regnstrom K, Ragnarsson EG, Koping-Hoggard M, Torstensson E, Nyblom H, Artursson P. PEI-a potent, but not harmless, mucosal immuno-stimulator of mixed T-helper cell response and FasL-mediated cell death in mice. Gene Ther 2003;10(18): 1575–83.
[28] Florea BI, Meaney C, Junginger HE, Borchard G. Transfection efficiency and toxicity of polyethylenimine in differentiated Calu-3 and nondifferentiated COS-1 cell cultures. AAPS PharmSci 2002;4(3):E12.
[29] Hunter AC. Molecular hurdles in polyfectin design and mechanistic background to polycation induced cytotoxicity. Adv Drug Deliv Rev 2006;58(14):1523–31.
[30] Ohba S, Ikeda T, Kugimiya F, Yano F, Lichtler A, Nakamura K, et al. Identification of a potent combination of osteogenic genes for bone regeneration using embryonic stem (ES) cell-based sensor. FASEBj 2007;21(8):1777–87.

My Technology

人工ウイルスの実現に向けた高分子ミセル型ベクターの設計

Design of Polymeric Micelle-based Non-viral Vectors Mimicking Natural Viruses

西山伸宏，片岡一則
Nobuhiro Nishiyama, Kazunori Kataoka

遺伝子治療において，技術面での鍵を握っているのは遺伝子の運び手（ベクター）の開発であり，安全性や製剤性に優れた非ウイルス型ベクターに対する期待が高まっている．このような非ウイルス型ベクターの開発において，天然の生命システムの構造と機能を理解し，その作動原理に啓発された機能の創り込みは，きわめて有効なアプローチである．本稿では，筆者らが開発を進めている高分子ミセル型ベクターに関して，細胞内の障壁とそれを乗り越えるための分子設計について紹介する．

key words 遺伝子治療，非ウイルス型ベクター，高分子ミセル

◉はじめに

遺伝子を"薬"として利用する遺伝子治療は，疾患メカニズムに基づいた分子治療として実用化が期待されているが，有効性と安全性を兼ね備えたベクターの開発が大きな課題となっている．これまでは，ウイルスベクターが広く利用されてきているが，免疫反応の惹起や取り扱いが困難であることなどの諸問題が存在し，その安全性を危惧する声も高まっていることから，医薬品としての実用化は容易ではないものと思われる．一方で，カチオン性脂質やカチオン性高分子（ポリカチオン）を構成要素とする非ウイルス型ベクター（non-viral vector）は，安全性，製剤性，生産コストなどに優れ，実用的なベクターとして期待されている．非ウイルス型ベクターは，全身投与による遺伝子デリバリーなどウイルスベクターでは困難な投与形態や治療応用が可能であり，核酸医薬として大きな注目を集めているsiRNAの送達システムとしても有望であるものと考えられている．しかしながら，非ウイルス型ベクターの遺伝子導入効率は必ずしも十分とは言えず，遺伝子導入に伴う細胞毒性の惹起など解決すべき課題が残されている．したがって，非ウイルス型ベクターの実用化のためには，その高性能化に向けた新しい分子設計や分子修飾が必要であり，ウイルスベクターはそのための良い教本となりうる．本稿では，筆者らが開発を進めている非ウイルス型ベクターである高分子ミセル型ベクターに関して，細胞内の障壁とそれを乗り越えるための分子設計について以下に概説する．

Ⅰ．ブロック共重合体の自己会合により形成される高分子ミセル型ベクター

ポリカチオンとDNAは，静電的相互作用によってナノスケールのDNA/ポリカチオン複合体（ポリプレックス）を形成することが知られており，*in vivo*応用が可能な非ウイルス型ベクターとして期待されている[1]．これに関連して，生体適合性高分子として知られるポリエチレングリコール（PEG）とポリカチオンが連結されたブロック共重合体は，DNAとの相互作用によってポリプレックス内核が高密度のPEG鎖で覆われた高分子ミセル型ベクターを形成する[2)-4)]（図1）．高分子ミセル型ベクターは，サイズの揃った数十nmの粒径を有しており，効果的に細胞内へと内在化され，内包DNA分子を加水分解や酵素分解から保護することができることから，さながら人工ウイルスと見なすことができる．また，

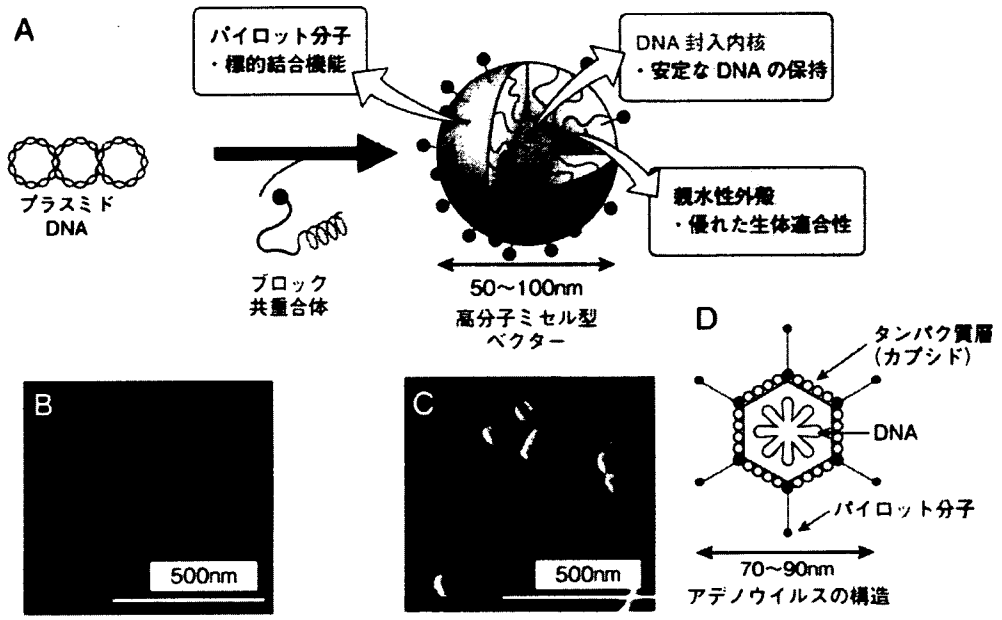

■図1 プラスミドDNAとPEG-ポリカチオンブロック共重合体の静電的相互作用によって形成される高分子ミセル型ベクター
プラスミドDNA(naked DNA)(B)に，ブロック共重合体を作用させることによって，100nm以下の単分散なトロイド状分子(C)に凝縮される．このようにして形成された高分子ミセル型ベクター(A)は，ウイルスベクター(D)を模倣した構造・機能の創り込みによって，高機能化が可能であり，生体に対して安全な人工ウイルスとして期待される．

高分子ミセル型キャリアは，抗癌剤を内包したシステムが，細網内皮系などの生体内異物排泄機構を回避することで血流中を長期滞留し，血管壁の透過性が亢進している固形癌に対して高い集積性と優れた治療効果を示すことから，その臨床治験が国内外で実施されており，全身投与のためのDNA送達システムとして有望である[4]．しかし，高分子ミセル型ベクターを細胞内で効率的に機能発現させるためには，細胞内の種々の障壁を乗り越えるための分子設計が必要である．

II．細胞による取り込み過程の制御

一般的に，ウイルスを含むナノ粒子は，エンドサイトーシスと呼ばれる小胞輸送によって細胞内に取り込まれるが，この過程には，クラスリン介在型，カベオレ介在型，マクロピノサイトーシスなどのいくつかの異なる経路が存在することが知られており，ウイルスの種類によってもこの経路が異なることが知られている[5](図2A)．このようなエンドサイトーシス経路の違いは，非ウイルス型ベクターの機能発現においてもきわめて重要であるものと考えられる．クラスリン介在型エンドサイトーシスでは，初期エンドソーム(pH6.0)→後期エンドソーム(pH5.0～6.0)→リソソーム(pH5.0～5.5)を経て，内包物は最終的に加水分解および酵素分解を受ける．したがって，非ウイルス型ベクターがこの経路によって取り込まれた場合は，エンドソームから細胞質内に脱出する機能が必要となる[6]．一方，カベオレ介在型エンドサイトーシスでは，カベオソームに移動し，エンドソームとは融合しないために，非ウイルス型ベクターは加水分解および酵素分解を受けないものと考えられる[7]．また，カベオソームは微小管を介して小胞体に輸送されることが報告されており[8]，非ウイルス型ベクターは核近傍に効率的に到達することができるために遺伝子発現に有利に働くものと考えられている[9]．マクロピノサイトーシスは，成長因子などのシグナルによって誘導され，比較的大きなマクロピノソームを形成し，最終的に細胞表面にリサイク

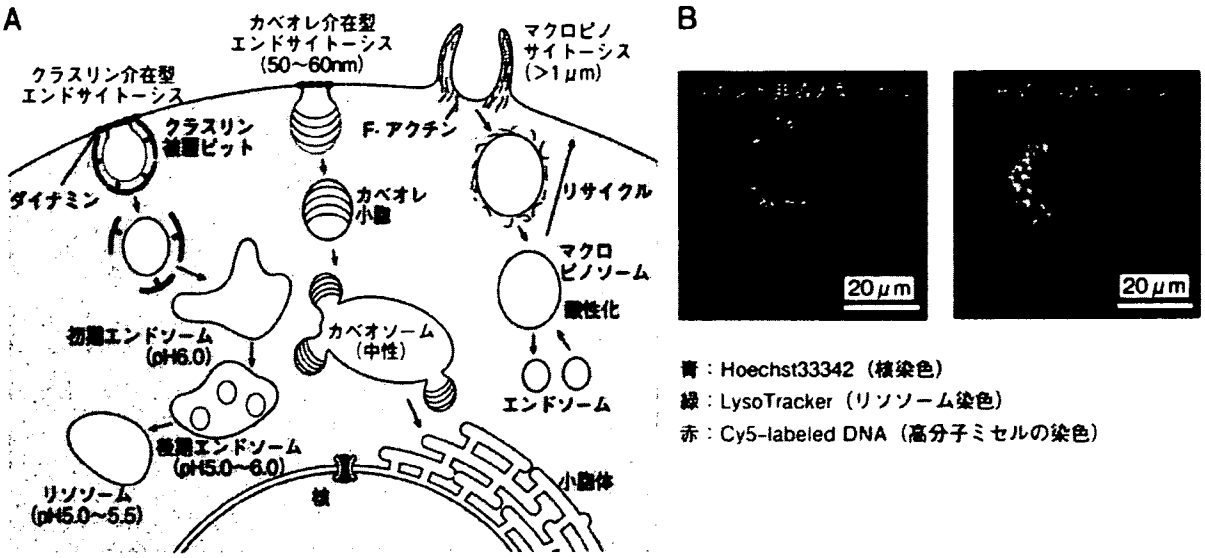

■図2 エンドサイトーシスによるナノ粒子の取り込み経路とcRGD導入型ミセルの細胞内局在
A：エンドサイトーシスによるナノ粒子の取り込み経路.
B：cRGD導入型ミセルの細胞内局在. Oba M, et al: Bioconjugate Chem (2007)18: 1415-1423より改変.

ルされる[10]. マクロピノソームは, エンドソームとの融合により酸性化するが, 他の輸送小胞と比較して内包物が漏れやすいと膜構造を有するものと考えられており, この経路も非ウイルス型ベクターの機能発現に有利であるものと思われる[11].

以上のような非ウイルス型ベクターのエンドサイトーシスによる取り込み経路は, 標的細胞の種類と, ベクターのサイズ, 表面特性(電荷, 親-疎水性など), リガンド分子の有無などに依存する. 近年, 筆者らは, 血管新生部位の血管内皮細胞や癌細胞において過剰発現が認められる$\alpha_v\beta_3$および$\alpha_v\beta_5$インテグリンに対して特異的に結合する環状RGD(cRGD)ペプチド(図3)[注1]を表面に導入した高分子ミセル型遺伝子ベクターを構築し, 蛍光標識DNAを用いてその細胞内分布を評価した[12][注2]. その結果, 3時間培養後, リガンド非導入型ミセルは細胞表面の近傍に局在した蛍光を示したが, cRGD導入型ミセルは核近傍にLysoTrackerによる染色とは一致しない蛍光を示したことから, cRGDの導入によって高分子ミセルは迅速に核近傍へと移動する一方で強い酸性条件には曝されていないことがわかった(図2B). さらに, cRGD導入型ミセルは, リガンド非導入型ミセルよりも有意に高い遺伝子導入効率を示すことも確認されている. 詳細なメカニズムの解明は今後の課題であるが, cRGD導入型ミセルはリガンド非導入型ミセルとは異なる細胞内輸送経路を示すことによって効率的な遺伝子発現を示した.

Ⅲ. 細胞質内への移行過程の制御

上述のようにエンドサイトーシスによって取り込まれた非ウイルス型ベクターが, 遺伝子発現を示すためには, エンドソームから細胞質内に脱出する必要がある. このようなエンドソーム脱出機能は, 天然のウイルスにも具備されている. 例えば, インフルエンザウイルスは, エンドソーム膜上に局在するヘマグルチニン(HA)がエンドソーム内の低pH環境下で開裂し, 疎水部が露出することでエンドソーム膜とエンドソーム膜の融合を惹起し, ウイルスゲノムを細胞質内に放出するものと考えられている. したがって, 非ウイルス型ベクターの開発においては, 細胞質内移行性を高めるための分子設計がきわめて重要である. ポリプレックスでは, いくつかのポリカチオンがエンドソーム脱出能を示すこと

注1
数あるインテグリンの中で$\alpha_v\beta_3$および$\alpha_v\beta_5$インテグリンを特異的に認識.

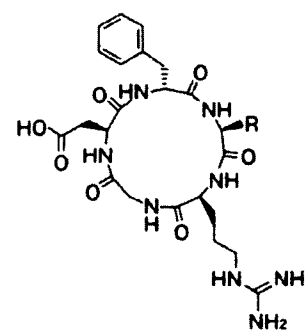

■図3 環状RGDペプチド

注2
〈実験条件〉
細胞：Hela細胞(30,000cells)
培養皿：35mm glass base dish
培地：1ml DMEM培地+10%血清
DNA量：3μg/dish
培養時間：3時間
顕微鏡：共焦点レーザー顕微鏡(Carl Zeiss LSM510)
対物レンズ：63倍

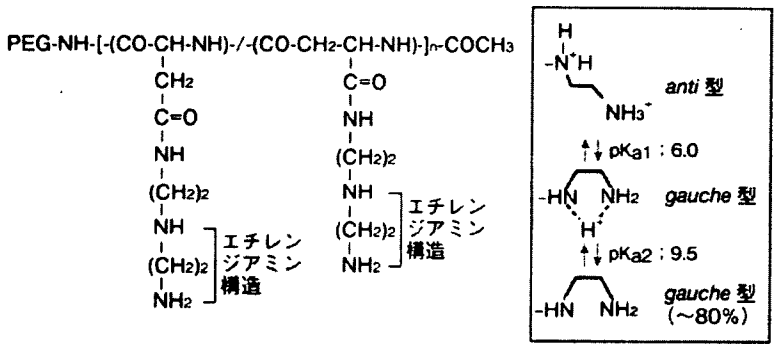

■図4 PEG-PAsp(DET)ブロック共重合体の化学構造

PEG-PAsp(DET)は，生理的pH7.4からエンドソーム内の酸性条件pH5.5に変化することによって，側鎖エチレンジアミン構造がモノプロトン状態(*gauche*型)からジプロトン状態(*anti*型)に変化し(赤枠内)，強力なバッファー能を発揮する．

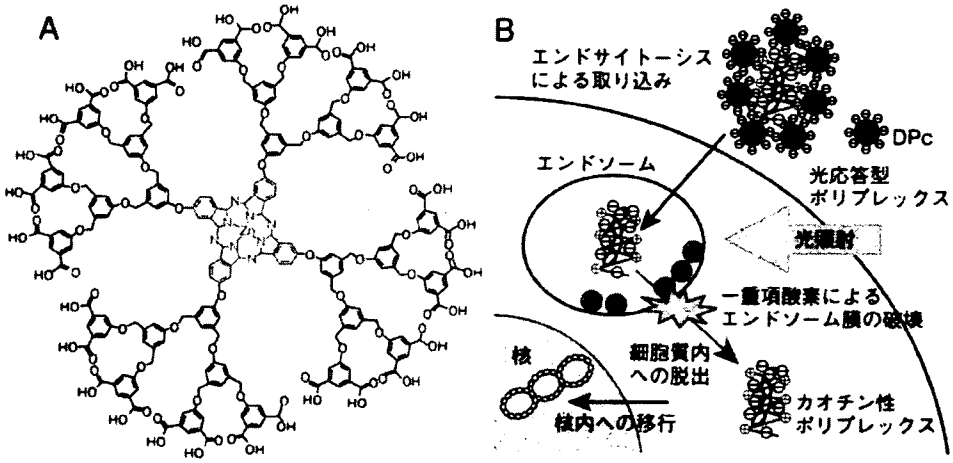

■図5 光に応答して機能発現する非ウイルス型ベクター(光応答型ポリプレックス)

A：アニオン性デンドリマーフタロシアニン(DPc)の化学構造．フタロシアニン(青)を中心色素とする樹状高分子(デンドリマー)であり，末梢にカルボキシル基を有するため，カチオン性のポリプレックスと静電的なコンプレックスを形成する．

B：光応答型ポリプレックスの光照射によるエンドソームから細胞質内への移行．

が報告されており，その中でポリエチレンイミン(PEI)が最も広く研究されている．このようなPEIのエンドソーム脱出能は，PEIが比較的低いpKaを有するために，エンドソーム内のpH低下を抑制するバッファーとして機能し，PEIのプロトン化に伴うイオン浸透圧の上昇によってエンドソーム膜が破壊されることに起因するものと考えられており，プロトンスポンジ効果として知られている[13]．

近年，筆者らは，側鎖カチオン構造の異なるPEG-ポリカチオンブロック共重合体を合成し，高分子ミセル型ベクターの遺伝子導入効率および細胞毒性に関してスクリーニングを行った[注3]．その結果，図4に化学構造を示したPEG-PAsp(DET)ブロック共重合体が，生理的pHからエンドソーム内の酸性条件に変化することによって，側鎖エチレンジアミン構造がモノプロトン状態からジプロトン状態に変化し，きわめて強力なバッファー能を発揮することで，プロトンスポンジ効果に基づくエンドソーム脱出により効率的な遺伝子発現を示すことが明らかとなった[14]．PEG-PAsp(DET)は，初代培養細胞への*in vitro*遺伝子導入や疾患モデルを用いた*in vivo*遺伝子導入において，既存のベクターよりも優位性が確認されており[15),16)注4]，今後の展開が期待される．

エンドソーム脱出は，ポリプレックスの遺伝子発現における最大の障壁の1つであるが，この過程を光などの外部エネルギーによって促進することができれば，生体内における遺伝子導入部位の制御が可能となる．そこで，筆者らは，近年，光応答性分子としてアニオン性のデンドリマーフタロシアニン(DPc：図5A)を搭載した非ウイルス型ベクターを開発した[17]．DPcは，細胞外環境においては，カチオン性のポリプレックスと静電的に相互作用するが，エンドソーム内の低pH環境下においては，末梢のカルボキシル基のプロトン化によって疎水化し，ポリプレックスから解離する一方で，エンドソーム膜と相互作用する．

注3

筆者らは，アミンの種類(1級アミン，2級アミン，3級アミン)と数およびスペーサーの長さの異なるポリカチオンを合成し，遺伝子導入効率と細胞毒性の観点からカチオン構造の最適化を行った．

注4

〈PEG-PAsp(DET)の優位性〉

①細胞毒性がきわめて低い[14]

②細胞の正常機能を阻害せず遺伝子導入による効率的な分化誘導などが可能(後述)[18]

③マウス頭頂骨の骨欠損モデルに対して骨誘導遺伝子の導入によって骨再生を確認[16]

④既存のベクターとは異なり，血小板の活性化や赤血球の凝集を惹起せず，動脈壁への遺伝子導入において血管を閉塞することなく効率的な遺伝子発現が得られることを確認[15]

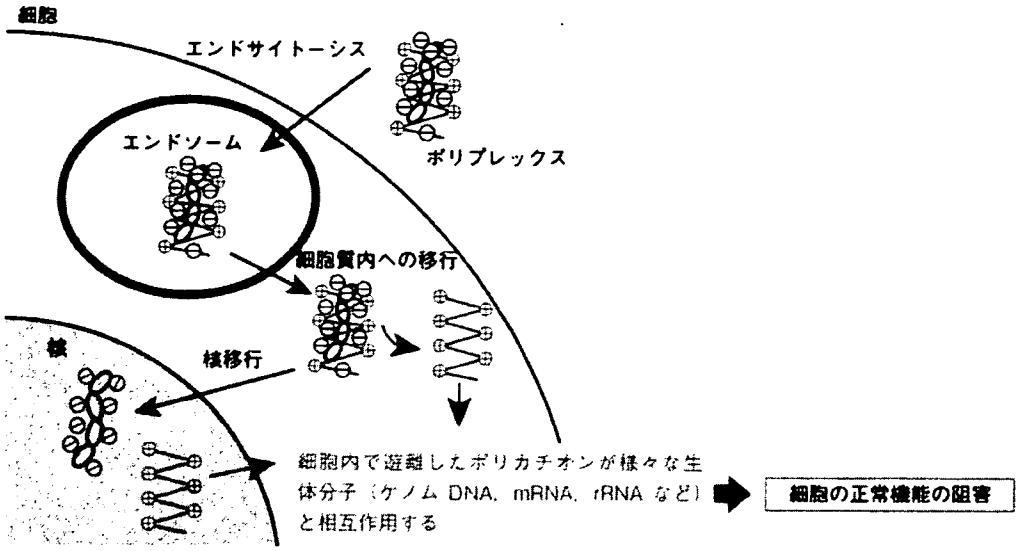

■図6 ポリプレックスを用いた遺伝子導入におけるポリカチオンの細胞機能に対する影響
ポリプレックスを構成するポリカチオンは，細胞内のアニオン性分子と相互作用し，細胞機能に影響を及ぼす可能性がある．

このとき，光照射を行うことによって，DPcより一重項酸素が産生され，エンドソーム膜が破壊されるために，ポリプレックスはエンドソームから細胞質内に脱出することができる（図5B）．その結果，この非ウイルス型ベクターは，光照射下で100倍以上の遺伝子発現を示し，ラット結膜への遺伝子導入実験において光照射部位に特異的な蛍光タンパク質の遺伝子発現を示した[17]．このようにエンドソーム脱出過程の制御によって，ウイルスベクターでは達成困難な遺伝子導入部位の制御が可能となった．

Ⅳ．ポリカチオンの細胞機能に対する影響

ポリプレックスを用いた遺伝子導入は，DNAと同時にポリカチオンを細胞質や核内に輸送するために，ポリカチオンが様々な細胞小器官やタンパク質と相互作用するものと考えられる．特に，ポリカチオンは，ゲノムDNA，RNA，rRNAなどの遺伝情報やその転写・翻訳を司る分子と相互作用する可能性があり，このような相互作用は細胞の正常機能に影響を及ぼすものと考えられる（図6）．そこで，近年，筆者らは，ポリカチオンとしてPAsp(DET)とPEIの細胞機能に与える影響について比較検討を行った[18]．その結果，PEIによる遺伝子導入は，内在性遺伝子およびハウスキーピング遺伝子の発現量ならびに細胞のポリプレックス取り込み活性を有意に低下させたが，PAsp(DET)による遺伝子導入では，そのような変化が確認されなかった．この原因は明らかではないが，PAsp(DET)では，pH7.4において側鎖エチレンジアミンが*gauche*型[注5]をとっており，このカチオン構造が生体に対して強い相互作用を示さないことに起因するものと思われる．また，両者のベクターを用いてGFPと分化誘導因子を細胞内に導入し，GFPと分化マーカーの遺伝子発現を評価したところ，両者のベクターは同等のGFP発現活性を示したが，PAsp(DET)を用いた場合のみに分化マーカーの顕著な遺伝子発現上昇が認められた[18]．すなわち，PEIは細胞の正常機能に影響を及ぼすために，分化誘導因子の発現にかかわらず，細胞は分化できないものと思われる．この結果は，遺伝子導入による細胞の機能制御において，遺伝子導入効率のみならずベクターの生体適合性がきわめて重要であることを示唆するものと考えられる．

注5
A-B-C-Dと結合している4つの原子について，B-C結合の回転に由来した立体配座の中で，A-B結合とC-D結合の二面角が60°の場合のものを指す．エチレンジアミンの場合，通常は*anti*型が安定ではあるが，エチレンジアミンのモノプロトン状態では2つのアミノ基の間でプロトンを共有することにより*gauche*型が安定となる．

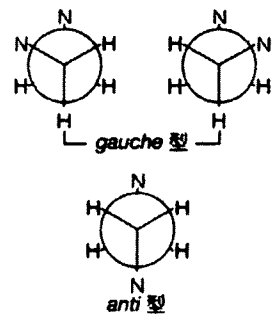

■図7 エチレンジアミンの*gauche*型および*anti*型

◉おわりに

本稿では，高分子ミセル型ベクターの設計に関して，細胞内への取り込み，細胞質内移行などに焦点を当てて概説したが，さらなる効率的な遺伝子発現を達成するためには，ベクターの核移行や転写効率などの向上もきわめて重要である．天然のウイルスの構造や機能を深く理解し，その作動原理に啓発された構造・機能を創り込んだ人工ウイルスを構築することによって，遺伝子治療が大きく進展するものと期待される．

PROFILE **西山伸宏**

■東京大学大学院医学系研究科 臨床医工学部門 講師
■E-mail：nishiyama@bmw.t.u-tokyo.ac.jp
■趣味：(男) 料理

2001年東京大学大学院工学系研究科博士後期課程修了(工学博士)．ユタ大学薬学部博士研究員，東京大学医学部附属病院助手，東京大学大学院医学系研究科助手を経て，2006年より現職．

PROFILE **片岡一則**

■東京大学大学院工学系研究科 マテリアル工学専攻 教授，医学系研究科 臨床医工学部門 教授
■E-mail：kataoka@bmw.t.u-tokyo.ac.jp
■趣味：スキー

1979年東京大学大学院工学系研究科博士後期課程修了(工学博士)．東京女子医科大学・助手-講師-助教授，東京理科大学基礎工学部助教授，教授を経て，1998年より現職(2004年より医学系研究科教授を併任)．

文献

1) Pack DW, et al: Nat Rev: Drug Discov (2005) 4: 581-593
2) Katayose S, et al: Bioconjugate Chem (1997) 8: 702-707
3) Itaka K, et al: Biomaterials (2003) 24: 4495-4506
4) Nishiyama N, et al: Pharmacol Ther (2006) 112: 630-648
5) Marsh M, et al: Cell (2006) 124: 729-740
6) Khalil IA, et al: Pharmacol Rev (2006) 58: 32-45
7) Pelkmans L, et al: Nat Cell Biol (2001) 3: 473-483
8) Mineo C, et al: Histochem Cell Biol (2001) 116: 109-118
9) Rejman J, et al: Mol Ther (2005) 12: 468-474
10) Swanson JA, et al: Trends in Cell Biol (1995) 5: 424-428
11) Khalil IA, et al: J Biol Chem (2006) 281: 3544-3551
12) Oba M, et al: Bioconjugate Chem (2007) 18: 1415-1423
13) Boussif O, et al: PNAS (1995) 92: 7297-7301
14) Kanayama N, et al: ChemMedChem (2006) 1: 439-444
15) Akagi D, et al: Gene Ther (2007) 14: 1029-1038
16) Itaka K, et al: Mol Ther (2007) 15: 1655-1662
17) Nishiyama N, et al: Nat Mater (2005) 4: 934-941
18) Masago K, et al: Biomaterials (2007) 28: 5169-5175

for beginners

・「先端生物医学研究・医療のための遺伝子導入テクノロジー ウイルスを用いない遺伝子導入法の材料，技術，方法論の新たな展開」田畑泰彦ら 編，遺伝子医学MOOK，メディカル ドゥ (2006)

GENE DELIVERY

Available online at www.sciencedirect.com
ScienceDirect
Journal of Controlled Release 122 (2007) 252–260
journal of controlled release
www.elsevier.com/locate/jconrel

PEG-based block catiomers possessing DNA anchoring and endosomal escaping functions to form polyplex micelles with improved stability and high transfection efficacy

Kanjiro Miyata [a,d], Shigeto Fukushima [b], Nobuhiro Nishiyama [c,d], Yuichi Yamasaki [b,d], Kazunori Kataoka [b,c,d,*]

[a] Department of Bioengineering, School of Engineering, The University of Tokyo, 7-3-1 Hongo, Bunkyo-ku, Tokyo 113-8656, Japan
[b] Department of Materials Engineering, School of Engineering, The University of Tokyo, 7-3-1 Hongo, Bunkyo-ku, Tokyo 113-8656, Japan
[c] Center for Disease Biology and Integrative Medicine, School of Medicine, The University of Tokyo, 7-3-1 Hongo, Bunkyo-ku, Tokyo 113-0033, Japan
[d] Center for NanoBio Integration, The University of Tokyo, 7-3-1 Hongo, Bunkyo-ku, Tokyo 113-8656, Japan

Received 26 May 2007; accepted 19 June 2007
Available online 27 June 2007

Abstract

For the development of polyplex systems showing a high transfection efficacy without a large excess of polycations, a lysine (Lys) unit as a DNA anchoring moiety was introduced into the amino acid sequence in poly(ethylene glycol)-*b*-cationic poly(*N*-substituted asparagine) with a flanking *N*-(2-aminoethyl)-2-aminoethyl group (PEG-*b*-Asp(DET)) resulting in PEG-*b*-P[Lys/Asp(DET)], in which the Asp(DET) unit acts as a buffering moiety inducing endosomal escape with minimal cytotoxicity. PEG-*b*-P[Lys/Asp(DET)]/DNA polyplexes exhibited a narrow size distribution of ~90 nm without secondary aggregates at the stoichiometric N/P 1, suggesting the formation of PEG-shielded polyplex micelles. The introduction of Lys units into the catiomer sequence facilitated cellular uptake and a 100-fold higher level of gene expression with PEG-*b*-P[Lys/Asp(DET)]/DNA polyplex micelles prepared even at a lowered N/P 2, possibly due to the enhanced association power of the anchoring Lys units.

Keywords: Gene delivery; PEG; Polyplex micelle; Block copolymer; Nonviral

1. Introduction

In recent years, enormous efforts have been devoted to the development of polycation-based gene delivery systems (polyplexes) due to their safety for clinical use, simplicity of preparation, and adaptability to large-scale production [1,2]. In particular, poly(ethylene glycol)-modified (PEGylated) polyplexes (polyplex micelles) formed through the electrostatic interaction between plasmid DNA (pDNA) and PEG-*b*-polycation copolymers (PEG-based block catiomers) are promising for *in vivo* gene therapy applications. The unique core-shell architecture of PEG-based block catiomers when combined with pDNA shows particle size data < 100 nm under physiological conditions [3]. Indeed, polyplex micelles from PEG-*b*-poly(L-lysine) copolymers showed a high colloidal stability in biological media, excellent biocompatibility, and prolonged circulation periods in the blood stream [4–6]. However, further improvement in the transfection efficacy of these polyplex systems is needed for translation into the clinic.

Previous studies have revealed that a high transfection efficacy was obtained from polycations with a relatively low p*K*a value, such as polyethylenimine (PEI), which is explained by their buffering effect in endosomal compartments, as described by the proton sponge hypothesis [7,8]. In this regard, we have developed PEG-*b*-poly(*N*-substituted asparagine) copolymers having the *N*-(2-aminoethyl)-2-aminoethyl group

* Corresponding author. Department of Materials Engineering, School of Engineering, The University of Tokyo, 7-3-1 Hongo, Bunkyo-ku, Tokyo 113-8656, Japan. Fax: +81 3 5841 7139.
E-mail address: kataoka@bmw.t.u-tokyo.ac.jp (K. Kataoka).

0168-3659/$ - see front matter © 2007 Elsevier B.V. All rights reserved.
doi:10.1016/j.jconrel.2007.06.020

in the side chain (PEG-*b*-PAsp(DET)). Consequently, these polyplex micelles exhibited a remarkably high transfection activity possibly due to the high buffering capacity based on the distinctive two-step protonation behavior of the flanking ethylenediamine moiety [9]. Also, we found that PEG-*b*-PAsp (DET) copolymers showed minimal cytotoxicity, allowing the successful transfection to primary cells [9–12]. However, an excess of PEG-*b*-PAsp(DET) copolymers with high N/P ratios were required for successful polyplex transfection; consequently, we concluded that micelle solutions prepared under such conditions are likely to contain a mixed population of: (i) block catiomers firmly condensing DNA, (ii) block catiomers loosely associated with DNA, and (iii) free or non-DNA condensing block catiomers. Hence, *in vivo* use of such PEG-*b*-PAsp(DET) polyplex micelles, particularly for systemic administration, may be limited, because loosely associated block catiomers easily desorb from the polyplex micelles during blood circulation, leading to the decreased transfection efficacy at the target site. Therefore, the micelle systems showing efficient transfection at lower N/P ratios without such non-associated or loosely associated catiomers should be next developed for *in vivo* gene delivery.

The present study was devoted to improving the transfection efficacy of the PEG-*b*-PAsp(DET)-based polyplex micelles at N/P ratios near unity by enhancing their association power through the introduction of Lys residues into the amino acid sequence of the block catiomer. Note that Lys residues are expected to anchor the associated block catiomers to the polyplex micelles. In this way, a significantly improved efficacy of transfection was achieved with the polyplex micelles with a subtle excess of block catiomers even after preincubation in the medium containing serum. This result seems to be associated with the facilitated cellular internalization of the polyplex micelles with stably incorporated block catiomers showing a high buffering capacity for endosomal escape.

2. Materials and methods

2.1. Materials

α-Methoxy-ω-amino-poly(ethylene glycol) (Mw 12,000) and β-benzyl-L-aspartate *N*-carboxyanhydride (BLA-NCA) were obtained from Nippon Oil and Fats Co., Ltd. (Tokyo, Japan). ε-(Benzyloxycarbonyl)-L-lysine *N*-carboxyanhydride (Lys(Z)-NCA) was synthesized from ε-(benzyloxycarbonyl)-L-lysine (Wako Pure Chemical Industries, Ltd., Osaka, Japan) by the Fuchs–Farthing method using bis(trichloromethyl) carbonate (triphosgene) (Tokyo Kasei Kogyo Co., Ltd., Tokyo, Japan) [13]. Diethylenetriamine (DET), *N,N*-dimethylformamide (DMF), dichloromethane, benzene, and trifluoroacetic acid were purchased from Wako Pure Chemical Industries, Ltd. Hydrogen bromide (HBr) (30% in acetic acid) was purchased from Tokyo Kasei Kogyo Co., Ltd. Branched polyethylenimine (25 kDa) (BPEI) was purchased from Sigma-Aldrich Co. (St. Louis, MO). The pDNA coding for *luciferase* with a CAG promoter (RIKEN, Japan) was amplified in competent DH5α *E. coli* and purified with a QIAGEN HiSpeed Plasmid MaxiKit (Germantown, MD). Luciferase Assay System Kit was purchased from Promega (Madison WI); Label IT Fluorescein Labeling Kit from Mirus Co. (Milwaukee, WI); and Micro BCA™ Protein Assay Reagent Kit from Pierce Co., Inc. (Rockford, IL).

2.2. Synthesis of PEG-b-P[Lys/Asp(DET)]

Block copolymers of PEG and L-lysine(Z)/β-benzyl-L-aspartate copolymer (P[Lys(Z)/BLA]), further referenced as PEG-*b*-P[Lys(Z)/BLA], were synthesized by ring-opening polymerization of a mixture of Lys(Z)-NCA and BLA-NCA initiated by the terminal primary amino group of α-methoxy-ω-amino-PEG (Scheme 1). The typical synthetic procedure is described as follows for the PEG-*b*-P[Lys(Z)/BLA] with 47 units of Lys(Z) and 52 units of BLA. Lys(Z)-NCA (1.29 g) and BLA-NCA (1.25 g) were dissolved in a mixture of DMF and dichloromethane (6.8 mL and 31.7 mL, respectively). This NCA solution was added to the PEG (1.0 g) in dichloromethane (15 mL) in a stream of dry argon and stirred at 35 °C for 48 h for copolymerization. The polymer in the reaction medium was precipitated in a mixture of hexane and ethyl acetate (600 mL and 400 mL, respectively), and purified by filtration. The acetylation of the *N*-terminal amino group of the obtained polymer (1.5 g) was subsequently performed at 35 °C for 1 h using acetic anhydride (500 μL) in a dichloromethane solution (22 mL). The polymer solution was precipitated into a mixture of hexane and ethyl acetate (300 mL and 200 mL, respectively), purified by filtration, and lyophilized from a benzene solution. The resulting copolymers had molecular weight distributions (Mw/Mn) of 1.1 to 1.3 as determined by GPC (data not shown). The degree of polymerization (DP) of the P[Lys(Z)/BLA] segment in the PEG-*b*-P[Lys(Z)/BLA] was determined from the peak intensity ratio of the methylene protons of PEG (OCH_2-CH_2, δ=3.5 ppm) to the aryl protons of the benzyl groups in the

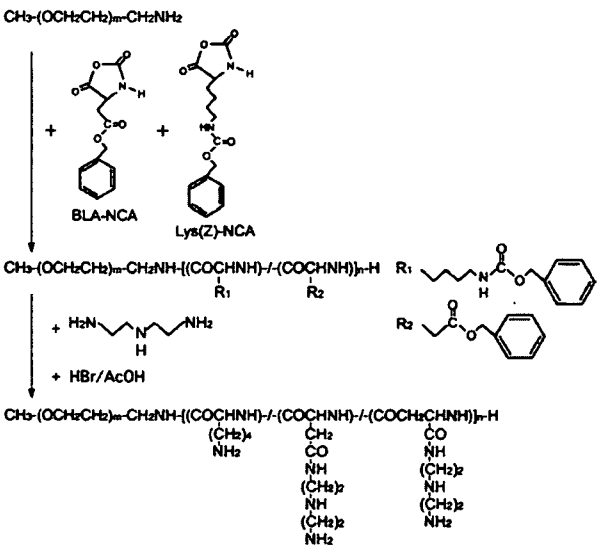

Scheme 1. Synthetic procedure of PEG-*b*-P[Lys/Asp(DET)].

Lys(Z) and BLA units (C_6H_6, δ=7.2–7.3 ppm) in the ^{1}H NMR spectra taken in dimethylsulfoxide at 80 °C. The compositions of the P[Lys(Z)/BLA] segments were determined from the peak intensity ratio of the protons of the β to δ methylene groups ($CH_2CH_2CH_2$, δ=1.2–2.0 ppm) in the side chain of the Lys(Z) units to the protons of the benzyl groups in the Lys(Z) and BLA units in the ^{1}H NMR spectra under the same conditions.

The PEG-*b*-P[Lys(Z)/BLA] copolymers (300 mg) were dissolved in DMF (6 mL), after which DET (2.5 mL; 50 eq to the benzyl group of PBLA) was added to the polymer solution, and stirred for 24 h at 40 °C under a dry argon atmosphere. After 24 h, the mixture was dropped into diethylether (120 mL) with stirring, and then the white precipitate was filtered and re-dissolved in trifluoroacetic acid (4 mL). To deprotect the Z group, HBr (30% in acetic acid) was then added and stirred for 1 h, after which the solution was dropped into diethylether (100 mL) with stirring, and the resulting precipitate was purified by filtered and dried *in vacuo*. The crude product was dissolved in distilled water, dialyzed against 0.01 N HCl and distilled water, and lyophilized to obtain the final product, PEG-*b*-P[Lys/Asp(DET)] as the hydrochloride salt form. The PEG-*b*-P[Lys/Asp(DET)] copolymers with varying ratios of Lys units to Asp (DET) units were obtained by changing the initial feeding ratio of Lys(Z)-NCA to BLA-NCA upon polymerization. The introduction of a DET moiety was confirmed from the peak intensity ratio of the methylene protons of PEG (OCH_2CH_2, δ=3.5 ppm) to the methylene protons of the introduced DET moieties ($CH_2CH_2NHCH_2CH_2$, δ=2.6–3.6 ppm) in the ^{1}H NMR spectra taken in D_2O at 25 °C.

2.3. Preparation of polyplex micelles from PEG-b-P[Lys/Asp (DET)]

The synthesized PEG-*b*-P[Lys/Asp(DET)] copolymer was dissolved in 10 mM Tris–HCl (pH 7.4) buffer at 5 mg/mL. This polymer solution was then mixed with pDNA in 10 mM Tris–HCl (pH 7.4) (50 μg/mL) at varying N/P ratios (residual molar ratio of amino groups in Lys and Asp(DET) units to pDNA phosphate groups), followed by a 24 h incubation at ambient temperature. The final concentration of pDNA in all the samples was adjusted to 33 μg/mL. The complexation of pDNA with the polycations was confirmed by agarose gel retardation analysis and ethidium bromide (EtBr) dye exclusion assay. In the gel retardation analysis, each sample was prepared by the dilution of the micelle solutions to the concentration of 8.3 μg pDNA/mL. 20 μL of each sample (166 ng pDNA) with a loading buffer was then electrophoresed at 100 V for 1 h on a 0.9 wt% agarose gel in 3.3 mM Tris–acetic acid buffer containing 1.7 mM sodium acetate. The migrated pDNA was visualized by soaking the gel in distilled water containing EtBr (0.5 μg/mL). In the EtBr dye exclusion assay, each sample (33 μg pDNA/mL) with varying N/P ratios was adjusted to 10 μg pDNA/mL with 2.5 μg EtBr/mL and 150 mM NaCl by adding 10 mM Tris–HCl (pH 7.4) buffer containing EtBr and NaCl. The solutions were incubated at ambient temperature overnight. The fluorescence intensity of the samples excited at 510 nm was measured at 590 nm and a temperature of 25 °C using a spectrofluorometer (Jasco, FP-777). The relative fluorescence intensity was calculated as follows:

$$F_r = (F_{sample} - F_0)/(F_{100} - F_0)$$

where F_{sample} is the fluorescence intensity of the micelle samples, F_{100} is the free pDNA, and F_0 is the background without pDNA.

2.4. Zeta-potential and dynamic light scattering (DLS) measurements

The zeta-potential of the polyplex micelles was determined from the laser-Doppler electrophoresis using the Zetasizer nanoseries (Malvern Instruments Ltd., UK) at a detection angle of 173° and a temperature of 25 °C. Each sample was prepared by simply mixing the polymer solutions with the pDNA solution at varying N^+/P ratios (33 μg pDNA/mL). The N^+/P ratio was defined as the residual molar ratio of protonated amino groups in PEG-*b*-P[Lys/Asp(DET)] to phosphate groups in DNA. The fraction of protonated amino groups in P[Lys/Asp(DET)] segment was calculated assuming that 100% and 50% of the amino groups in the Lys and Asp(DET) units, respectively, were protonated at pH 7.4 and a temperature of 25 °C based on the potentiometric titration results [9]. The samples were adjusted to 14 μg pDNA/mL by adding 10 mM Tris–HCl (pH 7.4) buffer, and then, injected into folded capillary cells (Malvern Instruments, Ltd.), followed by the measurement. From the obtained electrophoretic mobility, the zeta-potentials of each micelle were calculated by the Smoluchowski equation: $\zeta = 4\pi\eta\upsilon/e$ in which η is the viscosity of the solvent, υ is the electrophoretic mobility, and e is the dielectric constant of the solvent. The results are represented as the average of three experiments.

The sizes of each polyplex micelle were also measured by the DLS using the same apparatus. Micelle samples were prepared by mixing each polymer solution with pDNA solution at varying N^+/P ratios (33 μg pDNA/mL). After an overnight incubation at ambient temperature, the samples were adjusted to 14 μg pDNA/mL by adding 10 mM Tris–HCl (pH 7.4) buffer, and then injected into low volume glass cuvettes, ZEN2112 (Malvern Instruments, Ltd.), followed by the measurement. The data obtained from the rate of decay in the photon correlation function were analyzed by the cumulant method, and the corresponding hydrodynamic diameter of micelles was then calculated by the Stokes–Einstein equation [14].

2.5. Stability of polyplex micelles against counter polyanion exchange reaction

The stability of the polyplex micelle was estimated from the release of pDNA from the micelle caused by the exchange reaction with poly(aspartic acid) (PAsp, DP 66) as a polyanion. Ten mM Tris–HCl buffer (pH 7.4) solutions with varying concentrations of PAsp were added to the micelle solution with the pDNA concentration of 33 μg/mL. After overnight incubation at ambient temperature, each sample solution containing 167 ng of pDNA was electrophoresed through a 0.9 wt% agarose gel with

a running buffer of (3.3 mM Tris–acetic acid (pH 7.4)+1.7 mM sodium acetate+1 mM EDTA2Na). The pDNAs in the gel were visualized by soaking the gel into distilled water containing EtBr (0.5 mg/L).

2.6. Radiolabeling of pDNA for the cellular uptake study of polyplex micelles

pDNA was radioactively labeled with ^{32}P-dCTP using the Nick Translation System (Invitrogen, San Diego, CA). Unincorporated nucleotides were removed using High Pure PCR Product Purification Kit (Roche Laboratories, Nutley, NJ). After the purification, the 2 μg of labeled pDNA was mixed with 400 μg of non-labeled pDNA. The polyplex micelle samples were prepared by mixing the radioactive pDNA solution with each polymer solution (33 μg pDNA/mL). For cellular uptake experiments, Hela cells were seeded on 24-well cultured plates 24 h before the experiments in Dulbecco's modified Eagle medium (DMEM) containing 10% fetal bovine serum (FBS). The cells were incubated with 30 μL of the radioactive micelle solution (1 μg pDNA/well) in 400 μL of DMEM containing 10% FBS. After 24 h incubation, the cells were washed three times with Dulbecco's PBS and lysed with 400 μL of the cell culture Promega lysis buffer. The lysates were mixed with 5 mL of scintillation cocktail, Ultima Gold (PerkinElmer, MA), and then, the radioactivity of the lysate solution was measured by a scintillation counter. The results are presented as a mean and standard error of mean obtained from four samples.

2.7. In vitro transfection

Hela cells were seeded on 24-well culture plates and incubated overnight in 400 μL of DMEM containing 10% FBS. The medium was changed to 400 μL of fresh DMEM containing 10% FBS, and then 30 μL of each micelle solution was applied to each well (1 μg of pDNA/well). In the estimation of the effect of serum incubation on the transfection capacity of the micelle samples, the micelle solutions were preincubated with DMEM containing 10% FBS for 4 h and then added to the wells. After 24 h incubation, the medium was changed to 400 μL of fresh DMEM without micelle samples, followed by an additional 24 h incubation. The cells were washed with 400 μL of Dulbecco's PBS, and lysed by 100 μL of the cell culture Promega lysis buffer. The luciferase activity of the lysates was evaluated from the photoluminescence intensity using Mithras LB 940 (Berthold Technologies). The obtained luciferase activity was normalized with the amount of proteins in the lysates determined by the Micro BCA™ Protein Assay Reagent Kit (Pierce).

Table 1
A series of synthesized block cationers

Code	Feeding unit radio (Lys: Asp)	DP of poly (amino acid)	Unit number of Lys in poly(amino acid)	% of Lys units
L0/101	0:120	101	0	0
L24/102	25:90	102	24	24
L47/99	50:60	99	47	47
L70/98	75:30	98	70	71
L109/109	120:0	109	109	100

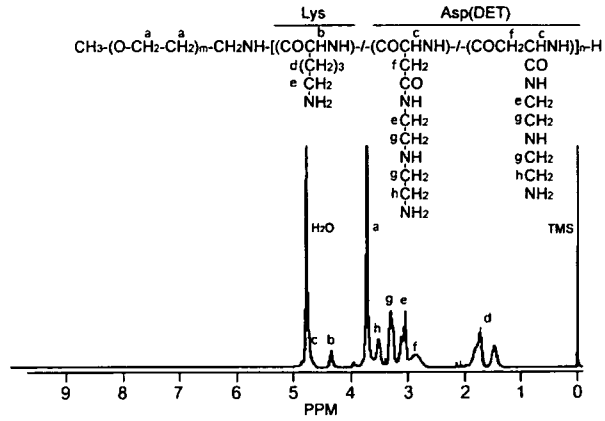

Fig. 1. ^{1}H-NMR spectrum of the PEG-*b*-P[Lys/Asp(DET)] (L47/99) (D_2O; 25 °C; concentration, 10 mg/mL).

2.8. Tolerability of polyplex micelles in serum-containing medium

The tolerability of polyplex micelles in serum-containing medium was estimated from the change in the fluorescence intensity of the fluorescein-labeled pDNA (F-pDNA) contained in the micelles. A pDNA was labeled using a Label IT Fluorescein Labeling Kit. This system promotes the covalent attachment of specific fluorescent molecules to guanine residues in nucleic acids. Each polyplex micelle sample was prepared by simply adding the polymer solution to the F-pDNA solution. After an overnight incubation at ambient temperature under dark conditions, the micelle solutions were mixed with 9 times volume of FBS solution, and then incubated at 37 °C for 4 h. The fluorescence emission of each sample excited at 492 nm was measured at 520 nm and a temperature of 37 °C using a spectrofluorometer (Jasco, FP-777). The obtained fluorescence intensities were expressed as the relative value to the fluorescence intensity of naked F-pDNA.

3. Results and discussion

3.1. Synthesis of PEG-b-P[Lys/Asp(DET)]

Block copolymers of PEG and P[Lys(Z)/BLA] (PEG-*b*-P[Lys(Z)/BLA]) were prepared by the ring-opening copolymerization of Lys(Z)- and BLA-NCAs as shown in Scheme 1. The poly(amino acid) segments with similar DP and varying Lys(Z)/BLA unit ratios were synthesized by changing the feeding ratio of Lys(Z)-NCA to BLA-NCA in the reaction mixture. The DPs and the unit ratios of Lys(Z)/BLA in the obtained copolymers were calculated from the peak intensity ratio in the ^{1}H NMR spectra (data not shown). As summarized in Table 1, five types of copolymers were prepared. The DP of the poly(amino acid) segments in a series of copolymers was confirmed to be approximately 100, regardless of the composition. These copolymers were then subjected to aminolysis reaction with DET, followed

by deprotection of the Z groups. The ^{1}H NMR spectra of the obtained catiomers, as typically seen in Fig. 1, reveal the quantitative aminolysis of BLA units as well as the complete deprotection of Lys(Z) units in the poly(amino acid) segment, because the methylene protons in the DET moiety and the β-methylene protons in the asparagine unit had a 4:1 peak intensity ratio and the peaks of the Z group disappeared in the ^{1}H NMR spectrum. These catiomers were abbreviated as L*x*/*y*, where *x* and *y* represent the unit number of Lys and the total DP of the poly(amino acid) segment, respectively.

3.2. Formation of polyplex micelles from PEG-b-P[Lys/Asp (DET)] catiomers

The polyplex micelles were prepared by simply mixing each catiomer solution with pDNA solution at varying N/P ratios. The complex formation of pDNA was confirmed by the agarose gel electrophoresis of each sample. With an increase in the N/P ratio, the amount of migrating free pDNA decreased, indicating the complex formation of pDNA with the PEG-*b*-P[Lys/Asp (DET)] catiomers (Supplementary Fig. 1). The critical N/P ratio where the migration of pDNA was completely retarded differed depending on the composition of the catiomers; i.e., the micelle of the block catiomers with a lower ratio of Lys units required the higher N/P ratio for the complete retardation of pDNA. To quantitatively evaluate the relationship between the N/P ratio and the condensation behavior of pDNA, the EtBr dye exclusion assay by fluorometry was completed. Fig. 2 (a) shows that the fluorescence intensity of EtBr decreased with an increase in the N/P ratio, and leveled off at a critical N/P ratio for each micelle system. These fluorescence data were then replotted against N^+/P ratio, the molar ratio of protonated amino groups at pH 7.4 in the block catiomers to phosphate groups in pDNA, as seen in Fig. 2 (b). Note that the ratios of the protonated amino groups in the block catiomer were calculated as 100% for Lys units and 50% for Asp(DET) units at pH 7.4, respectively, from the potentiometric titration results of PEG-*b*-PLys and PEG-*b*-PAsp(DET) block catiomers [9,15]. Interestingly, Fig. 2 (b) reveals that the fluorescence intensity of all the micelles leveled off at the N^+/P ratio of approximately 1 regardless of the composition of the catiomers, indicating that the condensation behavior of pDNA might be closely correlated with the ratio of charged groups (N^+/P). Also, this result strongly suggests that the PAsp(DET) segment in the micelles is likely to maintain the same protonation degree (α=0.5 at pH 7.4) as that in the free catiomer without the facilitated protonation by the complexation. As previously reported [9], this limited protonation for the proton sponge potential of the Asp(DET) units in the micelles is assumed to contribute to endosomal escape of PEG-*b*-P[Lys/Asp(DET)] polyplex micelles.

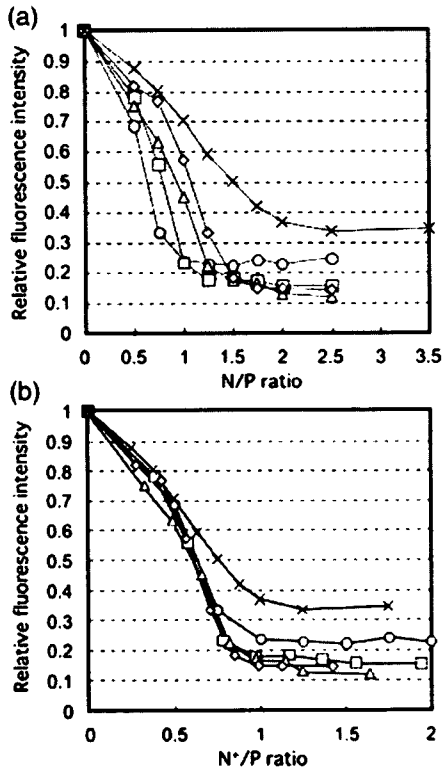

Fig. 2. EtBr dye exclusion assay on a series of polyplex micelles. Micelles included are: ×: L0/101; ◇: L24/102; △: L47/99; □: L70/98; ○: L109/109. (a) Relative fluorescence intensity vs. N/P ratio. (b) Relative fluorescence intensity vs. N^+/P ratio.

Fig. 3 (a) and (b) show the results obtained from DLS and zeta-potential measurements. The cumulant diameters of the polyplex micelles from the PEG-*b*-P[Lys/Asp(DET)]s were determined to be 70–100 nm throughout the range of the examined N^+/P > 1. As seen in the Fig. 3 (b) inset, the zeta-potentials of each polyplex micelle appear nearly neutral at an N^+/P 1, indicating the formation of the charge stoichiometric micelle from pDNA and the block catiomers. It should be emphasized that the polyplex micelles from PEG-*b*-P[Lys/Asp(DET)] had a narrowly distributed size of approximately 90 nm without secondary aggregates even at the charge neutralized condition (N^+/P 1) as previously demonstrated for those from PEG-*b*-PLys and PEG-*b*-PAsp(DET) catiomers [9,16]. It should also be noted that all polyplex micelles from the block catiomers had a much lower absolute value in zeta-potentials than polyplexes prepared from PAsp(DET) homopolymer (DP 98) (Fig. 3 (b)), possibly due to the shielding effect of the PEG layer surrounding the polyplex core. Nevertheless, there was a slight increase in the zeta-potentials of the polyplex micelles from neutral to positive values in the region of N^+/P > 1. This zeta-potential increase is likely to be ascribed to the loose association of excess catiomers with the polyplex micelles as previously reported for the PEG-poly(2-dimethylamino)ethyl methacrylate) catiomer/pDNA micelle [17]. Interestingly, the tendency of such increasing zeta-potentials with N^+/P ratios varied according to the composition of the block catiomers. The zeta-potential value of the polyplex micelles from PEG-*b*-PLys leveled off at an N^+/P 4 (+10 mV), while that from PEG-*b*-PAsp(DET) seemed to reach a plateau at a higher N^+/P 16 (+10 mV), suggesting that the association profile of the block catiomers with the polyplex micelles varied between PEG-*b*-PLys and PEG-*b*-PAsp(DET) micelles at N^+/P ratios ranging from 1 to 16. Presumably, PEG-*b*-PLys may reach the saturated association with pDNA at the lower

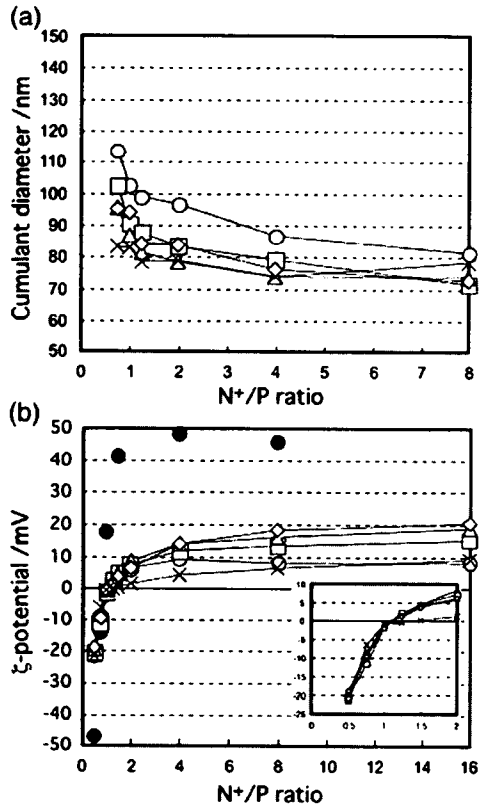

Fig. 3. (a) Size and (b) ζ-potential of a series of polyplex micelles and a PAsp (DET) polyplex. ×: L0/101 micelle, ◇: L24/102 micelle, △: L47/99 micelle, □: L70/98 micelle, ○: L109/109 micelle, ●: PAsp(DET) (DP 98) polyplex.

concentration (lower N^+/P) than PEG-*b*-PAsp(DET) due to the effective anchoring effect of the Lys units. Although PEG-*b*-P[Lys/Asp(DET)] micelles displayed the similar profiles of the zeta-potential to PEG-*b*-PLys micelles at lower N^+/P ratios, the micelles showed further increase in the surface charge in the range of $N^+/P > 4$ without leveling off. This result suggests that the association of PEG-*b*-P[Lys/Asp(DET)] with pDNA may not be saturated even in the range of $N^+/P > 4$, despite introduction of Lys units as a DNA anchoring moiety. This phenomenon may be ascribed to the unique structure of PEG-*b*-P[Lys/Asp(DET)] possessing two types of cationic units with different pDNA affinity. The presence of the Lys units in the block catiomer is likely to facilitate the binding of Asp (DET) units to pDNA, promoting the block catiomer association to the polyplex micelles at N^+/P 2 or lower; however, at high concentrations of the block catiomers (high N^+/P), Lys units may preferentially bind to the polyplex micelles to replace the Asp (DET) units, resulting in the continuous binding of the block catiomers until the Lys units saturate the available binding sites.

3.3. Stability of polyplex micelles

The result of the zeta-potential measurement suggested that the affinity of PAsp(DET) to pDNA seems to be enhanced by the incorporation of Lys units. The complexing stability of the polyplex micelles prepared from PEG-*b*-P[Lys/Asp(DET)] was evaluated directly from the standpoint of the counter polyion exchange reaction. The solutions with varying concentrations of PAsp were added to the solution of the PEG-*b*-PAsp(DET) micelle (N^+/P 2) in different A/P ratios (the molar ratio of carboxyl groups of PAsp to phosphate groups of pDNA). Consequently, the pDNA was released from the PEG-*b*-PAsp (DET) micelles at A/P > 3 due to the counter polyanion exchange of pDNA by PAsp (Fig. 4 (a)). In contrast, the improved stability of the polyplex micelles from PEG-*b*-P[Lys/Asp(DET)] was

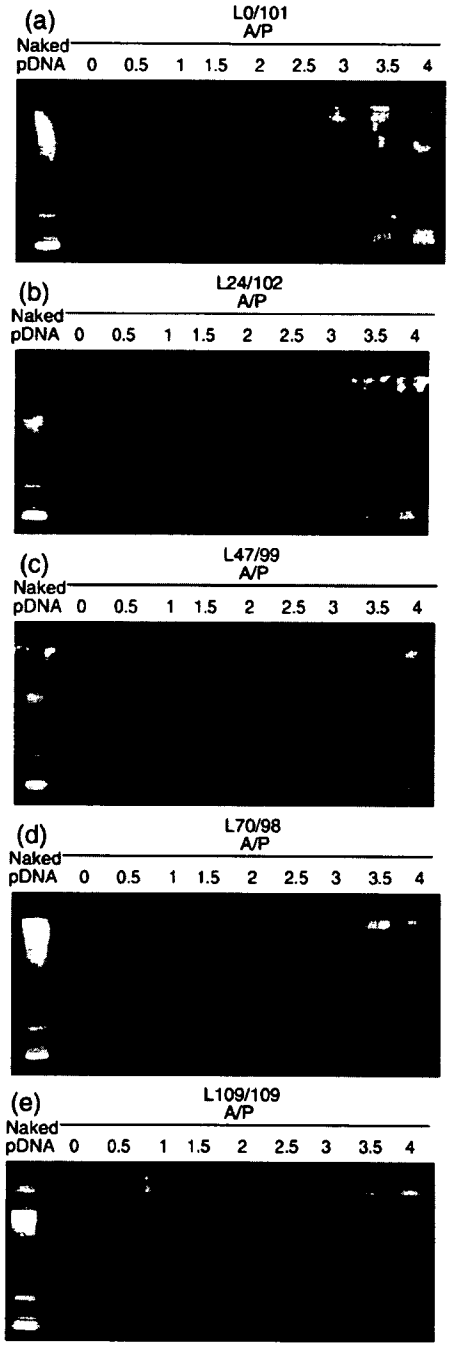

Fig. 4. Electrophoretic evaluation of polyplex micelle (N^+/P 2) tolerability against an exchange reaction with polyaspartic acid (DP 66). Note: A/P stands for the molar ratio of carboxyl groups in polyaspartic acid to phosphate groups in pDNA. Micelle samples prepared at N^+/P 2 were mixed with polyaspartic acid solution and electrophoresed after overnight incubation.

confirmed as shown in Fig. 4 (b)–(d): higher A/P ratios were required for the pDNA release with the increment in the percentage of Lys units in the amino acid sequence of the PEG-*b*-P[Lys/Asp(DET)]. In the case of the micelles from PEG-*b*-PLys, the pDNA release was not observed in the range of the examined A/P ratios (0–4) (Fig. 4 (e)). The similar tendency was also confirmed for the micelles prepared at N^+/P 4 (Supplementary Fig. 2). These results support our hypothesis that a Lys unit has a higher association power with pDNA than the Asp(DET) unit, and consequently, the PEG-*b*-P[Lys/Asp(DET)] micelles acquired the tolerability against the dissociation by polyanions through the anchoring effect of Lys units in the block catiomer.

3.4. Transfection with polyplex micelles from PEG-b-P[Lys/Asp(DET)]

Preliminary experiments on the cellular uptake of complexed pDNA revealed that the pDNA incorporated into PEG-*b*-PAsp (DET) at $N^+/P < 4$ was marginally internalized by cultured cells as is the case with naked pDNA (Supplementary Fig. 3). We speculate that this may contribute to the significantly lower transfection ability of PEG-*b*-PAsp(DET) micelles prepared at low N^+/P ratios. Herein, we hypothesize that the complexing stability promoted by the Lys anchors may facilitate the cellular uptake of polyplex micelles prepared even at low N^+/P ratios. To confirm this hypothesis, we completed a cellular uptake study using ^{32}P-radiolabeled pDNA. Fig. 5 reveals that the cellular uptake of pDNA complexed with block catiomers at an N^+/P ratio of 2 increased by the introduction of the Lys unit into the amino acid sequence. Especially, the polyplex micelles from the PEG-*b*-P[Lys/Asp(DET)] with the percentage of Lys units >47 exhibited more than a 10-fold uptake of pDNA compared to PEG-*b*-PAsp (DET). This result strongly suggests that the increased association power of the polyplex micelles may contribute to their facilitated cellular uptake without a large excess of block catiomers, i.e., at low N^+/P ratios. Interestingly, the cellular uptake of radioactive pDNA was maximized at the L70/98, even through its stability was deemed comparable to that of PEG-*b*-PLys (L109/109), as evidenced from the counter polyanion exchange reaction (Fig. 4

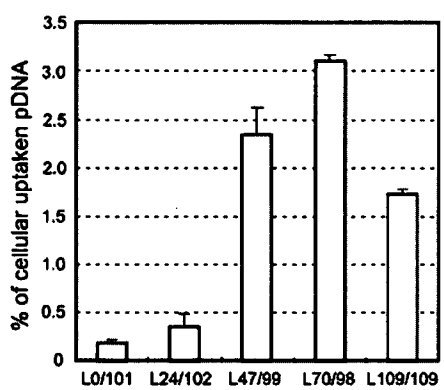

Fig. 5. The uptake of pDNA complexed with block catiomers at N^+/P 2 into Hela cells. ^{32}P-labeled pDNA micelles were incubated with the cells in DMEM containing 10% FBS at 37 °C for 24 h. The amount of internalized pDNA is represented as a percentage for the dosed pDNA (1 μg/well).

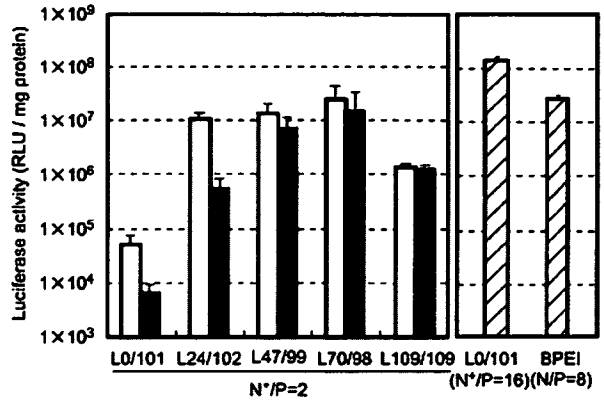

Fig. 6. *In vitro* transfection efficacy of polyplex micelles (N^+/P 2) against Hela cells. Open bars: Transfection efficacy without serum-preincubation. Closed bars: Transfection efficacy after 4 h incubation in the DMEM containing 10% FBS. Hatched bars: Transfection efficacy of the control; L0/101 micelles (N^+/P 16) and BPEI (25 kDa) polyplexes (N/P 8).

(d) and (e)). These data indicate that the increased cellular uptake of PEG-*b*-P[Lys/Asp(DET)] micelles compared to PEG-*b*-PLys micelles was not simply correlated to the enhanced stability. In this regard, a slightly positive zeta-potential of PEG-*b*-P[Lys/Asp (DET)] micelles compared to PEG-*b*-PAsp(DET) and PEG-*b*-PLys micelles is noteworthy, suggesting the surface charge may indeed affect the cellular uptake of the micelles with varying stabilities.

The effect of the introduction of the Lys unit as an anchoring moiety on the transfection ability of the polyplex micelles was then evaluated from the expression of a luciferase gene in the transfected cells. Although the PEG-*b*-PAsp(DET) micelles prepared at the high N^+/P 16 (ca. N/P 32) showed appreciably high transfection efficacy, which was one order of magnitude higher than that of BPEI polyplexes (25 kDa, N/P 8), reduction in the N^+/P ratio resulted in a sharp decline of the transfection ability of the PEG-*b*-PAsp(DET) micelles probably due to the lowered cellular uptake (Fig. 6). In contrast, the transfection efficacy could be maintained to be a high value even in the range of lowered N^+/P ratios by introducing Lys units into the block catiomer (Supplementary Fig. 4). Eventually, the PEG-*b*-P[Lys/Asp(DET)] micelles revealed an appreciably improved transfection efficacy at N^+/P 2 compared to the polyplex micelles of PEG-*b*-PLys and PEG-*b*-PAsp(DET) (Fig. 6, open bars). These results suggest that PEG-*b*-P[Lys/Asp(DET)] micelles may provide high stability and promote endosomal escape, presumably due to the synergistic effect of Lys and Asp(DET) units. The improved stability through the anchoring effect of Lys units was also confirmed from the transfection results after the preincubation of micelles in the serum-containing medium (Fig. 6, closed bars). The micelles from PEG-*b*-P[Lys/Asp(DET)], with the higher percentage of Lys units (L47/99 and L70/98), maintained the initial transfection capacity even after the serum-preincubation, whereas transfection efficacies of PEG-*b*-PAsp(DET) and L24/102 micelles, with a low percentage of Lys residues, were significantly impaired by serum-preincubation. These results strongly suggest that the associated block catiomers in the micelles from L47/99, L70/98, and L109/109 might be tolerable

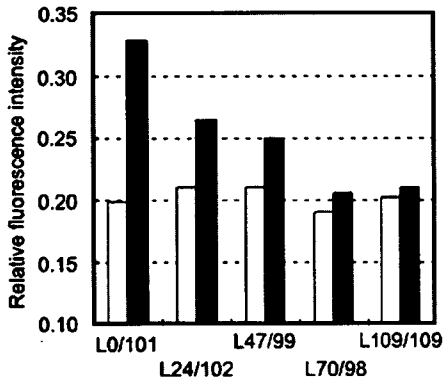

Fig. 7. Tolerability of polyplex micelles against serum incubation evaluated from the fluorescence recovery of the entrapped fluorescein-labeled pDNA due to serum-induced decondensation. Open bars: Fluorescence intensity in 10 mM Tris–HCl (pH 7.4) buffer solution without FBS. Closed bars: Fluorescence intensity after 4 h incubation in the medium containing 90% FBS.

in the transfection medium containing serum due to the strong anchoring of Lys units. This added strength of the Lys anchors is further supported by the sustained fluorescence quenching of fluorescein-labeled pDNA in micelles incubated in 90% FBS for 4 h as seen in Fig. 7. Apparently, fluorescence recovery due to the serum-inducing decondensation of pDNA was progressively inhibited with the increment in the percentage of Lys units in the PEG-*b*-P[Lys/Asp(DET)].

Although the transfection efficacy (Fig. 6) seems to be roughly correlated with the cellular uptake of the micelles (Fig. 5), careful examination reveals the tendency that the PEG-*b*-P[Lys/Asp(DET)] micelles with the lower percentage of Lys units, L24/102, achieved comparable transfection to those with the higher percentage of Lys units, 47/L98 and L70/98, even though the efficacy of pDNA uptake was fairly limited. This tendency becomes more apparent by normalizing the luciferase activity with pDNA uptake (Supplementary Fig. 5). This apparent increase in the transfection efficacy may be explained by the timely release of the loosely associated block catiomers from the micelles in the endosomal compartment to exert a high buffering capacity [9] and their possible interaction with the endosomal membrane component, facilitating the endosomal escape of the complexed pDNA, followed by a smooth release of pDNA directing efficient transcription. The loosely associated nature of L24/102 in the micelle may be supported from a decreased transfection efficacy after serum-preincubation as shown in Fig. 6.

4. Conclusion

Polyplex micelles from PEG-*b*-PAsp(DET) revealed a high transfection efficacy to various cell types including primary cells [9–12] presumably due to a low cytotoxicity and a strong pH-buffering capacity. Nevertheless, the weak association power of PAsp(DET) with DNA may be problematic for *in vivo* systemic administration, where the tolerability of polyplexes in proteinaceous media should be a crucial factor. Alternatively, a polylysine has an appreciably high affinity to DNA, however, the transfection efficacy of polylysine polyplexes remains low, possibly due to poor endosomal escaping functions and an impaired release of pDNA from the polyplex with an over-stabilized nature. In this novel study, we sought to alter these discrepancies by placing both Asp(DET) as a buffering unit with low cytotoxicity and Lys as a strong anchoring moiety to DNA in a single polymer strand resulting in PEG-*b*-P[Lys/Asp(DET)]. Polyplexes prepared from pDNA and PEG-*b*-P[Lys/Asp(DET)] have a micellar structure with a PEG palisade, exhibiting a remarkably improved stability compared to PEG-*b*-PAsp(DET)/pDNA polyplex micelles. PEG-*b*-P[Lys/Asp(DET)] polyplex micelles were further revealed to promote cellular internalization, leading to enhanced transfection efficacy even with a subtle excess of block catiomers. This enhanced transfection efficacy could be explained by the synergistic effect of Lys as an anchoring unit and Asp(DET) as a lower toxic endosomal escaping unit. This approach of placing cationic units with discriminating functions, e.g., DNA anchoring and endosomal escaping functions, into a single block catiomer strand is highly promising for future construct designs for effective *in vivo* systemic applications.

Acknowledgement

This work was financially supported by Research Fellowships of the Japan Society for the Promotion of Science for Young Scientists (JSPS), the Mitsubishi Chemical Corporation Fund, and the Core Research Program for Evolutional Science and Technology (CREST) from the Japan Science and Technology Corporation (JST). The authors express their appreciation to Dr H. Hamada (RIKEN, Japan) for providing the plasmid DNA.

Appendix A. Supplementary data

Supplementary data associated with this article can be found, in the online version, at doi:10.1016/j.jconrel.2007.06.020.

References

[1] D.W. Pack, A.S. Hoffman, S. Pun, P.S. Stayton, Design and development of polymers for gene delivery, Nat. Rev. Drug Discov. 4 (2005) 581–593.
[2] E. Mastrobattista, M.A.E.M. van der Aa, W.E. Hennink, D.J.A. Crommelin, Artificial viruses: a nanotechnological approach to gene delivery, Nat. Rev. Drug Discov. 5 (2006) 115–121.
[3] K. Kakizawa, K. Kataoka, Block copolymer micelles for delivery of gene and related compounds, Adv. Drug Deliv. Rev. 54 (2002) 203–222.
[4] K. Itaka, A. Harada, K. Nakamura, H. Kawaguchi, K. Kataoka, Evaluation by fluorescence resonance energy transfer of the stability of nonviral gene delivery vectors under physiological conditions, Biomacromolecules 3 (2002) 841–845.
[5] M. Harada-Shiba, K. Yamauchi, A. Harada, I. Takamisawa, K. Shimokado, K. Kataoka, Polyion complex micelles as a vector in gene therapy-pharmacokinetics and in vivo gene transfer, Gene Ther. 9 (2002) 407–414.
[6] K. Miyata, Y. Kakizawa, N. Nishiyama, Y. Yamasaki, T. Watanabe, M. Kohara, K. Kataoka, Freeze-dried formulations for in vivo gene delivery of PEGylated polyplex micelles with disulfide crosslinked cores to the liver, J. Control. Release 109 (2005) 15–23.
[7] O. Boussif, F. Lezoualc'h, M.A. Zanta, M.D. Mergny, D. Scherman, B. Demeneix, J.-P. Behr, A versatile vector for gene and oligonucleotide transfer into cells in culture and in vivo: Polyethylenimine, Proc. Natl. Acad. Sci. U. S. A. 92 (1995) 7297–7301.

[8] M. Neu, D. Fischer, T. Kissel, Recent advances in rational gene transfer vector design based on poly(ethylene imine) and its derivatives, J. Gene Med. 7 (2005) 992–1009.
[9] N. Kanayama, S. Fukushima, N. Nishiyama, K. Itaka, W.-D. Jang, K. Miyata, Y. Yamasaki, K. Kataoka, PEG-based biocompatible block catiomer with high-buffering capacity for the construction of polyplex micelles showing efficient gene transfer toward primary cells, ChemMedChem 1 (2006) 439–444.
[10] D. Akagi, M. Oba, H. Koyama, N. Nishiyama, S. Fukushima, T. Miyata, H. Nagawa, K. Kataoka, Biocompatible micellar nanovectors achieve efficient gene transfer to vascular lesions without cytotoxicity and thrombus formation, Gene Ther. 14 (2007) 1029–1038.
[11] M. Han, Y. Bae, N. Nishiyama, K. Miyata, M. Oba, K. Kataoka, Transfection study using multicellular tumor spheroids for screening non-viral polymeric gene vectors with low cytotoxicity and high transfection efficiencies, J. Control. Release, in press.
[12] K. Itaka, S. Ohba, K. Miyata, H. Kawaguchi, K. Nakamura, T. Takato, U. Chung, K. Kataoka, Bone regeneration by regulated in vivo gene transfer using biocompatible polyplex nanomicelles, Mol. Ther., in press.
[13] W.H. Daly, D. Poche, The preparation of *N*-carboxyanhydrides of alpha-amino-acids using bis(trichloromethyl)carbonate, Tetrahedron Lett. 29 (1988) 5859–5862.
[14] A. Harada, K. Kataoka, Formation of polyion complex micelles in an aqueous milieu from a pair of oppositely-charged block-copolymers with poly(ethylene glycol) segments, Macromolecules 28 (1995) 5294–5299.
[15] A. Harada, S. Cammas, K. Kataoka, Stabilized α-helix structure of poly (L-lysine)-block-poly(ethylene glycol) in aqueous medium through supramolecular assembly, Macromolecules 29 (1996) 6183–6188.
[16] K. Itaka, K. Yamauchi, A. Harada, K. Nakamura, H. Kawaguchi, K. Kataoka, Polyion complex micelles from plasmid DNA and poly(ethylene glycol)-poly(L-lysine) block copolymer as serum-tolerable polyplex system: physicochemical properties of micelles relevant to gene transfection efficiency, Biomaterials 24 (2003) 4495–4506.
[17] D. Wakebayashi, N. Nishiyama, K. Itaka, K. Miyata, Y. Yamasaki, A. Harada, H. Koyama, Y. Nagasaki, K. Kataoka, Polyion complex micelles of pDNA with acetal-poly(ethylene glycol)-poly(2-(dimethylamino(ethyl methacrylate) block copolymer as the gene carrier system: Physicochemical properties of micelles relevant to gene transfection efficacy, Biomacromolecules 5 (2004) 2128–2136.